# Design, synthesis, and electrophysiological evaluation of NS6740 derivatives: exploration of the structure-activity relationship for alpha7 nicotinic acetylcholine receptor silent activation

Maria Chiara Pismataro [a, b, c], Nicole A. Horenstein [b], Clare Stokes [c], Marta Quadri [a, b, c], Marco De Amici [a], Roger L. Papke [c], Clelia Dallanoce [a, *]

[a] *Department of Pharmaceutical Sciences, Medicinal Chemistry Section "Pietro Pratesi", University of Milan, Via L. Mangiagalli 25, 20133 Milan, Italy*
[b] *Department of Chemistry, University of Florida, P.O. Box 117200, Gainesville, FL 32611-7200, USA*
[c] *Department of Pharmacology and Therapeutics, University of Florida, P.O. Box 100267, Gainesville, FL 32610-0267, USA*

---

*Keywords:*
α7 nicotinic acetylcholine receptor
Electrophysiology
Silent agonist
Partial agonist
1,4-Diazabicyclo[3.2.2]nonane
Structure-activity relationship (SAR)

---

*Abbreviations:* ACh, acetylcholine; CAP, cholinergic anti-inflammatory pathway; diEPP, 1,1-diethyl-4-(phenyl)piperazin-1-ium iodide; $D_i$, PAM-insensitive nonconducting desensitized state; $D_s$, PAM-sensitive nonconducting desensitized state; DMAP, 4-(dimethylamino)pyridine; DME, 1,2-dimethoxyethane; GAT107, (3a*R*,4*S*,9b*S*)-4-(4-bromophenyl)-3a,4,5,9b-tetrahydro-3*H*-cyclopenta[c]quinoline-8-sulfonamide; GTP, guanosine triphosphate; $H_{n+2}P_nO_{3n+1}$, polyphosphoric acid; $IP_3$, inositol triphosphate; nAChR, nicotinic acetylcholine receptor; NS6740, 1,4-diazabicyclo[3.2.2]nonan-4-yl(5-(3-(trifluoromethyl)-phenyl)-furan-2-yl)methanone; *p*-$CF_3$-diEPP, 1,1-diethyl-4-(4-(trifluoromethyl)phenyl)piperazin-1-ium iodide; PAM, positive allosteric modulator; $Pd(PPh_3)_4$, tetrakis(triphenylphoshine)palladium(0); PNU-120596, *N*-(5-chloro-2,4-dimethoxyphenyl)-*N'*-(5-methyl-3-isoxazolyl)-urea; s, second; SARs, structure–activity relationships; SEM, standard error of the mean; TEA, triethylamine; TNF-α, tumor necrosis factor-α; triEMA, triethylmethylammonium; TsCl, tosyl chloride.

* Corresponding author.
*E-mail address:* clelia.dallanoce@unimi.it (C. Dallanoce)

## A B S T R A C T

The α7 nicotinic acetylcholine receptor (nAChR) silent agonists, able to induce receptor desensitization and promote the α7 metabotropic function, are emerging as new promising therapeutic anti-inflammatory agents. Herein, we report the structure–activity relationship investigation of the archetypal silent agonist NS6740 (1,4-diazabicyclo[3.2.2]nonan-4-yl(5-(3-(trifluoromethyl)-phenyl)-furan-2-yl)methanone) (**1**) to elucidate the ligand-receptor interactions responsible for the α7 silent activation. In this study, NS6740 fragments **11**-**16** and analogs **17**-**32** were designed, synthesized, and assayed on human α7 nAChRs expressed in *Xenopus laevis* oocytes with two-electrode voltage clamping experiments. All together the structural portions of NS6740 were critical to engender its peculiar activity profile. The diazabicyclic nucleus was essential but not sufficient for inducing α7 silent activation. The central hydrogen-bond acceptor core and the aromatic moiety were crucial for promoting prolonged α7 receptor binding and sustained desensitization. Compounds **13** and **17** were efficacious partial agonists. Compounds **12**, **21**, **23**-**26**, and **30** strongly desensitized α7 nAChR and therefore may be of interest for additional investigation of inflammation responses. We gained key structural information useful for further silent agonist development.

## 1. Introduction

The α7 nicotinic acetylcholine receptor (nAChR) is a ligand-gated ion channel composed of five identical α7 subunits, and it is the second most abundant nAChR subtype in the human brain, where it mainly exists in the hippocampus, cerebral cortex, and other regions associated with learning, memory, and cognition [1−4]. The α7 nAChR is also expressed in the peripheral nervous system and in tissues and cells that are not associated with neuronal function [5,6]. The α7 subtype exhibits unique physiological and pharmacological properties, including high calcium permeability, rapid desensitization, fast onset and decay kinetics, and a very low probability of channel opening [7,8]. The distinctive α7 activation and desensitization have been investigated in the presence and absence of the α7 type II positive allosteric modulator (PAM) *N*-(5-chloro-2,4-dimethoxyphenyl)-*N'*-(5-methyl-3-isoxazolyl)-urea (PNU-120596), and two major forms of α7 desensitization have been identified [9]. The desensitized $D_i$ state is insensitive to the PAM, whereas the $D_s$ state is sensitive to and destabilized by PNU-120596 and other type II PAMs. The $D_s$ state is probably associated with the rapid form of desensitization unique to α7 that is connected to channel open states in presence of type II modulators. Several electrophysiological and calcium imaging studies, together with the analysis of mutant receptors have shown the ability of α7 nAChRs to operate both via canonical ionotropic cation influx through the open-channel state, which due to the high calcium permeability of the channel can lead to calcium-induced calcium release, and via non-conventional metabotropic channel signaling, possibly through direct $G_q$ protein coupling that promotes the inositol triphosphate ($IP_3$)-mediated calcium release [10−13]. In neurons, both ionotropic and metabotropic α7 functions have been observed, and it has been suggested that a structural transition of the channel opening induced by agonist ligand binding enables a metabotropic signaling states which seem to coincide with channel desensitization [14,15]. However, the metabotropic α7 signal transduction behavior is most relevant in cell types such as immune cells, where receptor-mediated ion currents are not observed [16,17]. Indeed, the α7 nAChR modulates the release of pro-inflammatory cytokines from monocytes, microglia, and macrophages. These anti-inflammatory effects are not due to classical channel activation through ionotropic conductance [18,19]; rather, for this receptor a large interactome was identified, members of which may trigger the ability to operate metabotropically [20]. Based on mutational studies, a G protein-binding region within the M3-M4 loop has been implicated to be responsible for a direct coupling of the α7 nAChR to GTP-binding proteins, which enables a downstream calcium signaling response that can persist beyond the expected time course of α7 channel activation [21]. In microglia for example, the α7 nAChRs attenuate neuroinflammation and regulate TNF-α release through the interaction with the heterotrimeric G protein subunit α ($G\alpha_i$) signaling pathway [22].

A significant number of studies indicate that α7 nAChR-dependent signals can be activated via vagus nerve stimulation as part of the cholinergic anti-inflammatory pathway (CAP), leading to regulation of cytokine production and related tissue injury response, supporting the idea that CAP is a robust physiological mechanism [23]. It is interesting to consider that α7-activating nicotinic agents might be used as molecular tools to investigate CAP activity and prevent or modulate the development of cytokine-mediated diseases. The distinction between ionotropic and metabotropic receptor activities becomes essential to the development of therapeutics targeting α7 nAChRs, and efforts should be made to identify compounds that are able to selectively regulate α7 function [24]. In this direction, there is a growing interest in silent agonists [25−32], a class of ligands that promote entry of the receptor into a desensitized state with respect to ionotropic activity. Thus they may represent an alternative therapeutic strategy to modulate anti-inflammatory responses [20,25−27]. A number of α7 silent agonists have been described so far: NS6740 (**1**) [28], KC-1 (**2**) [29], (*R*)-47 (**3**) [30], triEMA (**4**) [31], TEA (**5**) [31], diEPP (**6**) [31] and its analog *p*-$CF_3$-diEPP (**7**) [27,32], the sulfonium salt **8** [33], the spirocyclic quinuclidine **9** and its analogues [34], and the quinuclidine oxadiazole ammonium salt **10** [35] (Fig. 1). Silent agonists are able to induce receptor desensitization that responds to type II PAMs [9]. In the absence of PAMs, silent agonists appear to operate almost entirely through the metabotropic mode and exert little or no ionotropic activity.

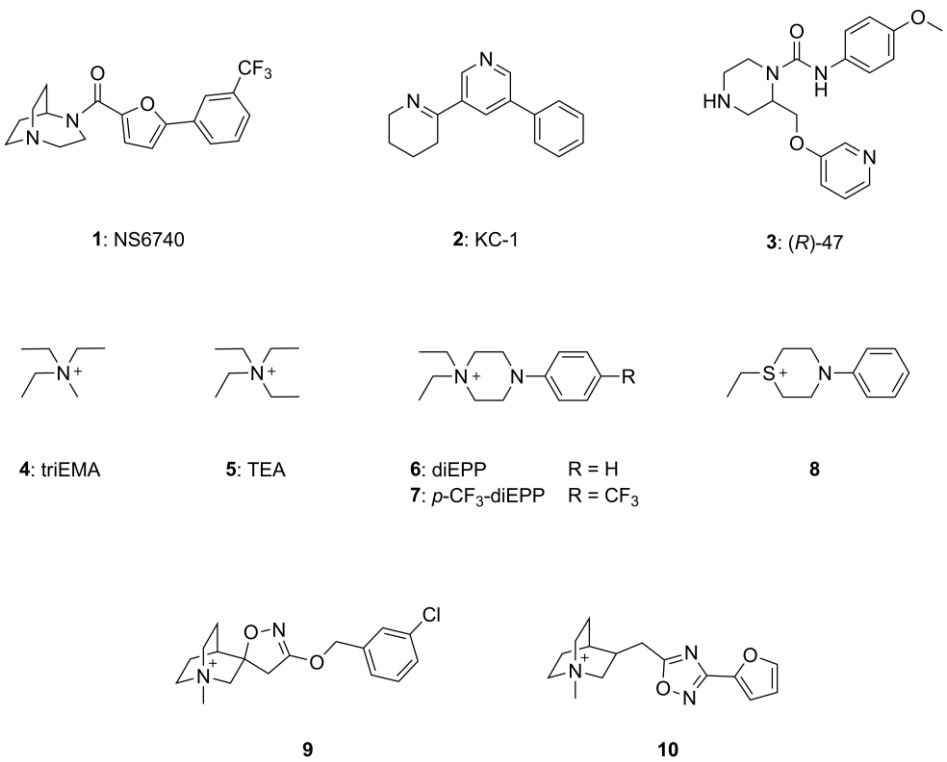


**Fig. 1.** Structures of known α7 nAChR silent agonists.

The archetypal silent agonist 1,4-diazabicyclo[3.2.2]nonan-4-yl(5-(3-(trifluoromethyl)-phenyl)-furan-2-yl)methanone (NS6740, **1**, Fig. 1) was first published in a model study for cognitive improvement, in which it not only failed to enhance avoidance learning but antagonized the effects of an efficacious α7 agonist. Although **1** displayed little efficacy at α7 nAChR when applied alone, its agonist properties were revealed in combination with the type II PAM PNU-120596 [28]. Indeed, NS6740 is a very weak partial agonist that produces little channel activation on its own but has been shown to stabilize long-lived nonconducting receptor states that are sensitive to activation by allosteric modulators ($D_s$). The α7 receptor desensitization induced by NS6740 is so remarkably prolonged that when the PAM was applied alone to the receptor after NS6740, the effect persisted even after an hour of washout from the bath [36]. NS6740 is one of the most promising anti-inflammatory compounds to target the α7 nAChR. It has been proven to reduce the lipopolysaccharide-stimulated secretion of tumor necrosis factor-α (TNF-α) from rat cultured microglia [19] and is also effective in reducing inflammation in mouse models of peripheral neuropathy and tonic inflammatory pain [26]. The time and concentration dependence of these analgesic effects is consistent with NS6740 induction of non-conducting receptor states, thus indicating that signaling pathways required for anti-inflammatory responses are fulfilled by α7 receptors in the desensitized conformation [26].

The structure of NS6740 shows a protonatable nitrogen atom within the 1,4-diazabicyclo[3.2.2]nonane system, a hydrogen-bond acceptor heterocyclic moiety, and an aromatic ring (Fig. 2B). Data suggest that the silent binding site is an extension of the orthosteric binding site [31,36]; however, some aspects of the ligand-receptor interaction for α7 silent modulation are yet to be clarified. Additionally, recent data [37] have indicated that some silent agonists may bind to an extracellular allosteric site, shared with ago-PAMs like GAT107 that can couple to the transmembrane PAM site to produce PAM-dependent activation of receptors in the $D_s$ states. The pharmacophoric features of NS6740, which are common to other silent agonists (Fig. 1), make NS6740 capable of generating multiple interactions in the silent agonist binding sites, allowing long lasting effects on the conformational equilibrium of receptor states.

Expanding our previous research on the α7 nAChRs [29,31−46], we broadly investigated the structure-activity relationships (SARs) of the lead structure **1** with the goal to elucidate the pharmacophore features for silent agonism and the ligand-receptor interactions that are able to induce the α7 desensitized states. Human α7 nAChRs were expressed in *Xenopus laevis* oocytes, and two electrode voltage clamping was employed to establish the electrophysiological profile of the new compounds in the absence and presence of a type II PAM. We determined channel activation, inhibition of acetylcholine (ACh) responses after the compounds were applied alone, and responses potentiated by the PAM PNU-120596. These insights would allow the design of new compounds which may be useful for future studies to deepen the α7 metabotropic signaling

and to selectively target the inflammatory responses derived from this non-conventional α7 function, while importantly minimizing the ionotropic activity.

## 2. Results and Discussion

### *2.1. Design*

On this ground, we synthesized NS6740 fragments (compounds **11-16**) (Fig. 2A) and analogs (compounds **17-32**) (Fig. 2B) to deduce SARs associated with their electrophysiological properties, paying particular attention to the propensity of compounds to desensitize the receptor with minimal channel activation.

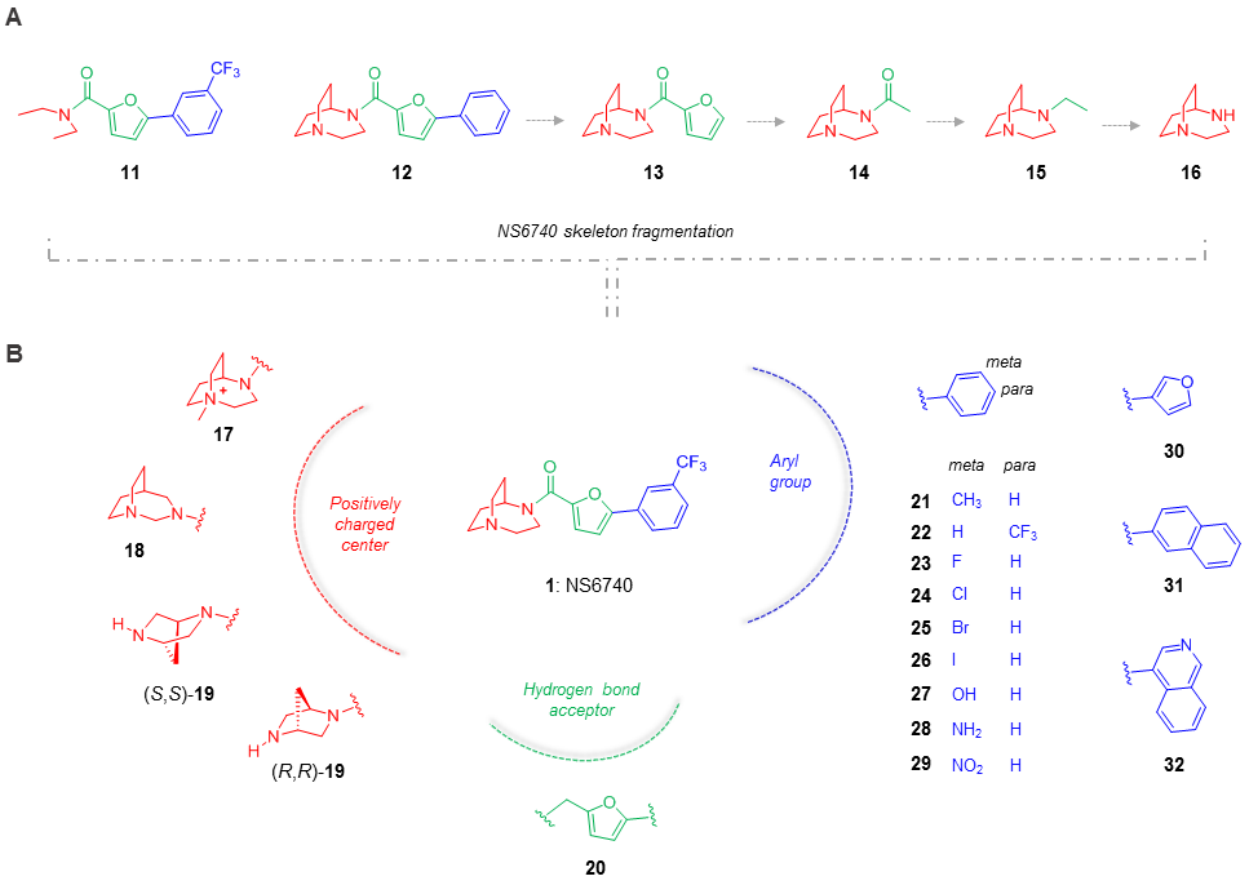


**Fig. 2.** Chemical modifications performed on the lead compound NS6740 (**1**). (**A**) Structures of compounds **11-16** derived from NS6740 skeleton fragmentation. (**B**) New compounds **17-32** obtained by manipulations on the three NS6740 pharmacophoric substructures.

Following a fragmentation approach, the NS6740 skeleton was dissected in molecular portions (**11-16**, Fig. 2A) to clarify the influence of each structural element and confirm the proposed

pharmacophore interaction features. We synthesized compound **11**, lacking the diazabicyclic system, to evaluate the role of the protonatable nitrogen atom. Furthermore, we prepared compounds **12-16**, characterized by progressive removal of structural parts, i.e. trifluoromethyl group (**12**), phenyl ring (**13**), furan nucleus (**14**), carbonyl function (**15**), and ethyl chain (**16**), which could imply loss or impairment of crucial interactions with the silent binding site. Fragments **15** and **16** retain the positively charged moiety as the only residual pharmacophore element. Then, for an alternate SAR study, we designed and synthesized a series of novel NS6740 analogs (compounds **17-32**, Fig. 2B), focusing on structural modifications of the three pharmacophoric portions of its scaffold. Concerning the investigation of the NS6740 positively charged center, we examined the effect of quaternization at the 1,4-diazabicyclo[3.2.2]nonane nitrogen atom tertiary amine (**17**) since the permanent charge could generate stronger ionic interactions and lead to different conformational receptor states. Then the regioisomeric 1,3-diazabicyclo[3.2.2]nonane system (**18**) was introduced to evaluate how the distance between the positively charged nitrogen and the carbonyl group could influence the proper ligand orientation responsible for inducing receptor desensitization. We also investigated the different spatial and electrostatic interactions due to the smaller enantiomeric (*S*,*S*)- and (*R*,*R*)-2,5-diazabicyclo[2.2.1]heptane nucleus ((*S*,*S*)-**19** and (*R*,*R*)-**19**)), characterized by a secondary amine nitrogen. Focusing next on the central portion of NS6740 with hydrogen bonding capability, we explored the contribution of the carbonyl group by removing it in derivative **20**. Lacking the amide bond, this modification introduced also more flexibility into the NS6740 together with an additional protonatable nitrogen atom. Finally, we explored chemical modifications of the pharmacophoric aryl moiety, initially focusing on the *meta*-substitution. The influence of the trifluoromethyl group was evaluated by replacement with its bioisosteric methyl group (**21**) and by shifting it from the *meta* to *para* position (**22**). The trifluoromethyl group was also replaced by fluorine (**23**), chlorine (**24**), bromine (**25**), and iodine (**26**), to assess the effect of halogen atoms with increasing size. The influence of polar substituents, such as hydroxy (**27**), amino (**28**), and nitro (**29**) groups, was investigated as well. Then we tested the replacement of the trifluoromethyl phenyl moiety by the heterocyclic furan ring (**30**) and by bulky aromatic groups, namely naphthalene (**31**) and isoquinoline (**32**), to explore the effect of the increased steric hindrance on ligand-receptor interactions.

### *2.2. Chemistry*

The diazabicyclic systems **16** and **37** were synthesized by applying minor changes and optimizations to a patented procedure [47] (Scheme 1). The commercially available 3-quinuclidinone hydrochloride **33** was reacted with hydroxylamine, and the resulting oxime **34**

underwent Beckmann rearrangement upon treatment with polyphosphoric acid at 130 °C to give the lactam regioisomers **35** and **36**, which were then separated by silica gel column chromatography and obtained in a 6:1 ratio. Reduction with lithium aluminum hydride yielded the diazabicyclic derivatives **16** and **37** which, due to their volatility, were isolated as dihydrochlorides after treatment with a 4 M solution of hydrochloric acid in 1,4-dioxane.

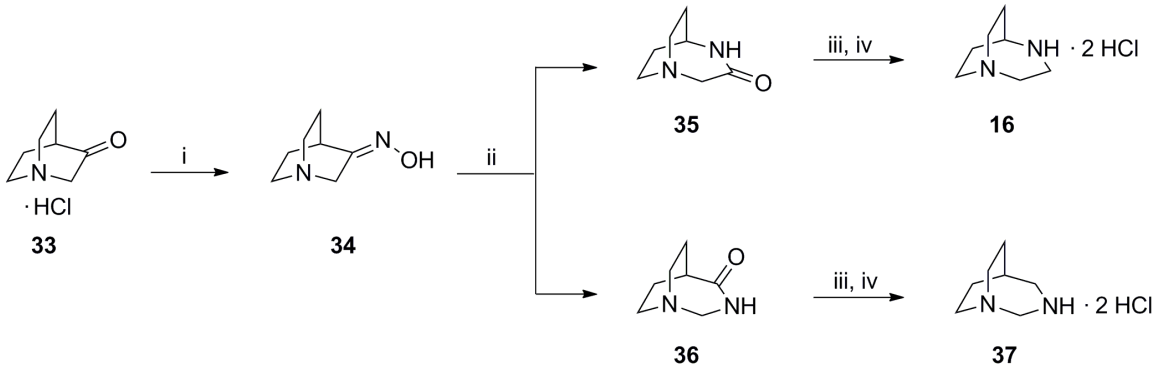


**Scheme 1.** Synthesis of diazabicyclic systems **16** and **37**. Reagents and conditions: (i) $NH_2OH{\cdot}HCl$ (1.15 equiv), $CH_3COONa$ (3 equiv), $H_2O$, 70 °C, 2 h; (ii) $H_{n+2}P_nO_{3n+1}$, 130 °C, 20 h; (iii) 1 M $LiAlH_4$ in THF (1.2 equiv), 0 °C to reflux, 8 h; (iv) 4 M HCl in 1,4-dioxane (2 equiv), rt, overnight.

The synthesis of the two enantiomeric diazabicyclic systems (*S*,*S*)-**43** and (*R*,*R*)-**43** was performed according to Scheme 2 in a similar manner as described earlier [48]. *Trans*-4-hydroxy-L-proline (2*S*,4*R*)-**38** was *N*-tosylated by reaction with tosyl chloride in the presence of sodium carbonate to produce intermediate (2*S*,4*R*)-**39**, which was reduced with borane in THF, leading to the corresponding diol (2*S*,4*R*)-**40**. Subsequent ditosylation of (2*S*,4*R*)-**40** in the presence of DMAP in pyridine afforded the tritosyl derivative (2*S*,4*R*)-**41** together with ditosylchloromethyl side product (ratio about 3:1), which were separated by silica gel column chromatography. The cyclization of (2*S*,4*R*)-**41** was achieved with benzylamine in MeOH heated in a sealed tube at 90 °C to form the (1*S*,4*S*)-2-benzyl-5-tosyl-2,5-diazabicyclo[2.2.1]heptane (*S*,*S*)-**42**. Treatment of (*S*,*S*)-**42** with hydrobromic acid in acetic acid allowed cleavage of the tosyl group and led to the diazabicyclic moiety (*S*,*S*)-**43**. The enantiomer (*R*,*R*)-**43** was prepared starting from *cis*-4-hydroxy-D-proline (2*R*,4*R*)-**44**, which was converted to methyl ester (2*R*,4*R*)-**45** as the hydrochloride by esterification with aqueous hydrochloric acid in methanol at reflux. Ditosylation of (2*R*,4*R*)-**45** in pyridine at 0 °C in the presence of trimethylamine, followed by configurational inversion of the 4-hydroxy moiety of ditosyl intermediate (2*R*,4*R*)-**46** with tetraethylammonium acetate tetrahydrate in toluene under refluxing conditions, provided the 4-acetyl derivative (2*R*,4*S*)-**47**. Saponification of (2*R*,4*S*)-**47** in THF with a 0.5 M aqueous potassium hydroxide solution at room temperature directly afforded the *N*-tosyl-*trans*-4-hydroxy-D-proline (2*R*,4*S*)-**39**, which is the enantiomer of compound (2*S*,4*R*)-**39**. We obtained the (1*R*,4*R*)-2-benzyl-2,5-diazabicyclo[2.2.1]heptane (*R*,*R*)-**43** by carrying intermediate (2*R*,4*S*)-**39** through the same reaction sequence as that described for

(2*S*,4*R*)-**39** (Scheme 2).

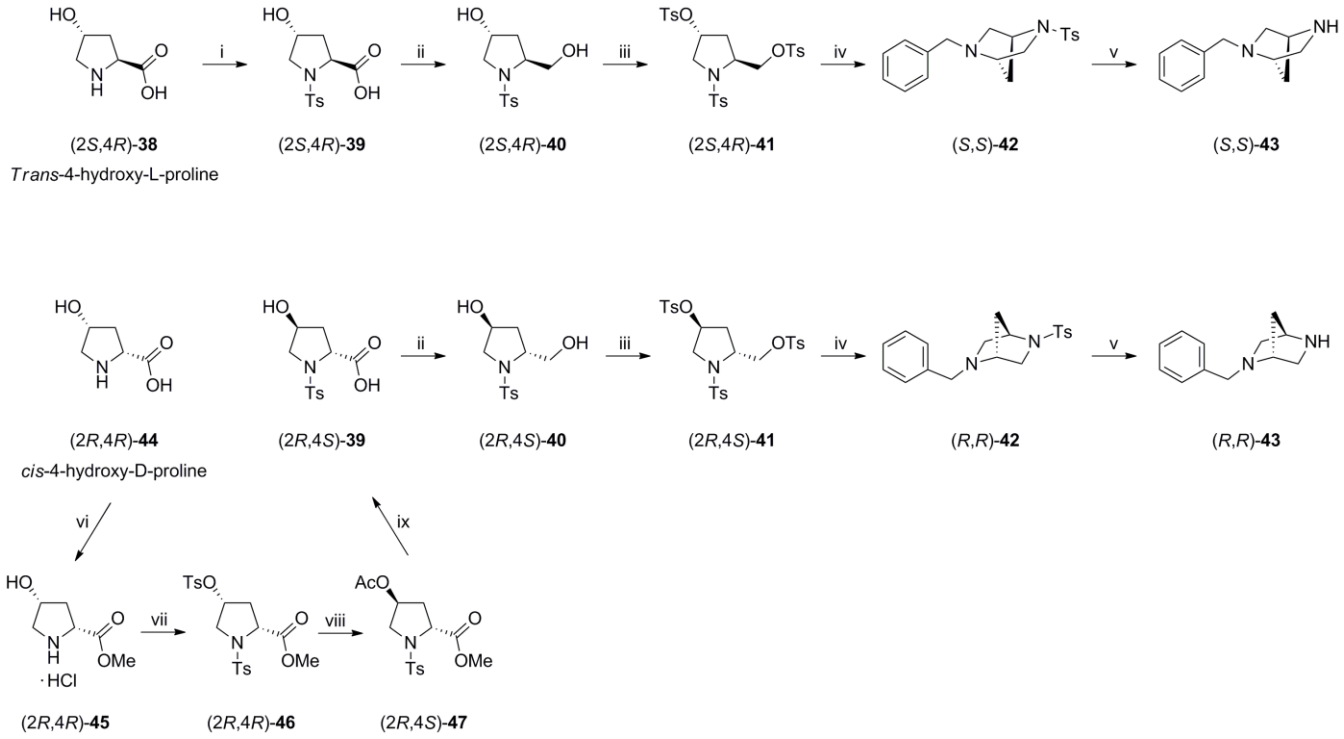


**Scheme 2.** Synthesis of enantiomeric diazabicyclic systems (*S*,*S*)-**43** and (*R*,*R*)-**43**. Reagents and conditions: (i) TsCl (1.2 equiv), $Na_2CO_3$ (2.1 equiv), $H_2O$, 0 °C to rt, 48 h; (ii) 1 M $BH_3$·THF complex (2–3 equiv), anhydrous THF, 0 °C to rt, 6–15 h; (iii) TsCl (2–5 equiv), anhydrous pyridine (4.8 equiv), DMAP (0.2 equiv), anhydrous $CH_2Cl_2$, 0 °C to rt, 24 h; (iv) benzylamine (10 equiv), MeOH, 90 °C, overnight; (v) 33% HBr/AcOH, 50 °C, 2–5 h; (vi) 1.25 M HCl in MeOH, 0 °C to reflux, 6 h; (vii) TsCl (6.6 equiv), anhydrous pyridine, $Et_3N$ (3 equiv), 0 °C, 15 h; (viii) tetraethylammonium acetate tetrahydrate (1.3 equiv), anhydrous toluene, reflux, 4 h; (ix) 0.5 M KOH in $H_2O$ (5 equiv), THF, rt, 3 h.

The synthetic route for the preparation of the 5-arylfuran-2-carbonyl chloride intermediates **62a-m** and **63-65** is outlined in Scheme 3. Methyl 5-bromofuran-2-carboxylate **49** was prepared by refluxing the commercially available 5-bromofuran-2-carboxylic acid **48** with concentrated sulfuric acid in methanol. To introduce the planned aromatic substituents, intermediate **49** was treated with different commercially available aryl boronic acids **50a-g**, **50i**, **50l**, **51-53** under Suzuki-Miyaura cross-coupling reaction conditions, using tetrakis(triphenylphoshine)palladium(0) as the catalyst in the presence of sodium carbonate in dimethoxyethane or dimethylformamide to afford compounds **54a-g**, **54i**, **54l**, **55-57** in 60-90% yield [49]. Due to the reactivity of iodine in Suzuki conditions, intermediate **54h** was prepared from the amino derivative **54l** in a one-pot procedure via diazonium salt followed by substitution with potassium iodide [50]. Subsequent saponification of **54a-l**, **55-57** yielded the 5-arylfuran-2-carboxylic acid intermediates **58a-l**, **59-61**, which, in addition to the commercial *meta*-nitro phenyl compound **58m**, were treated with thionyl chloride at reflux to give the corresponding carbonyl

chloride derivatives **62a-m**, **63-65**.

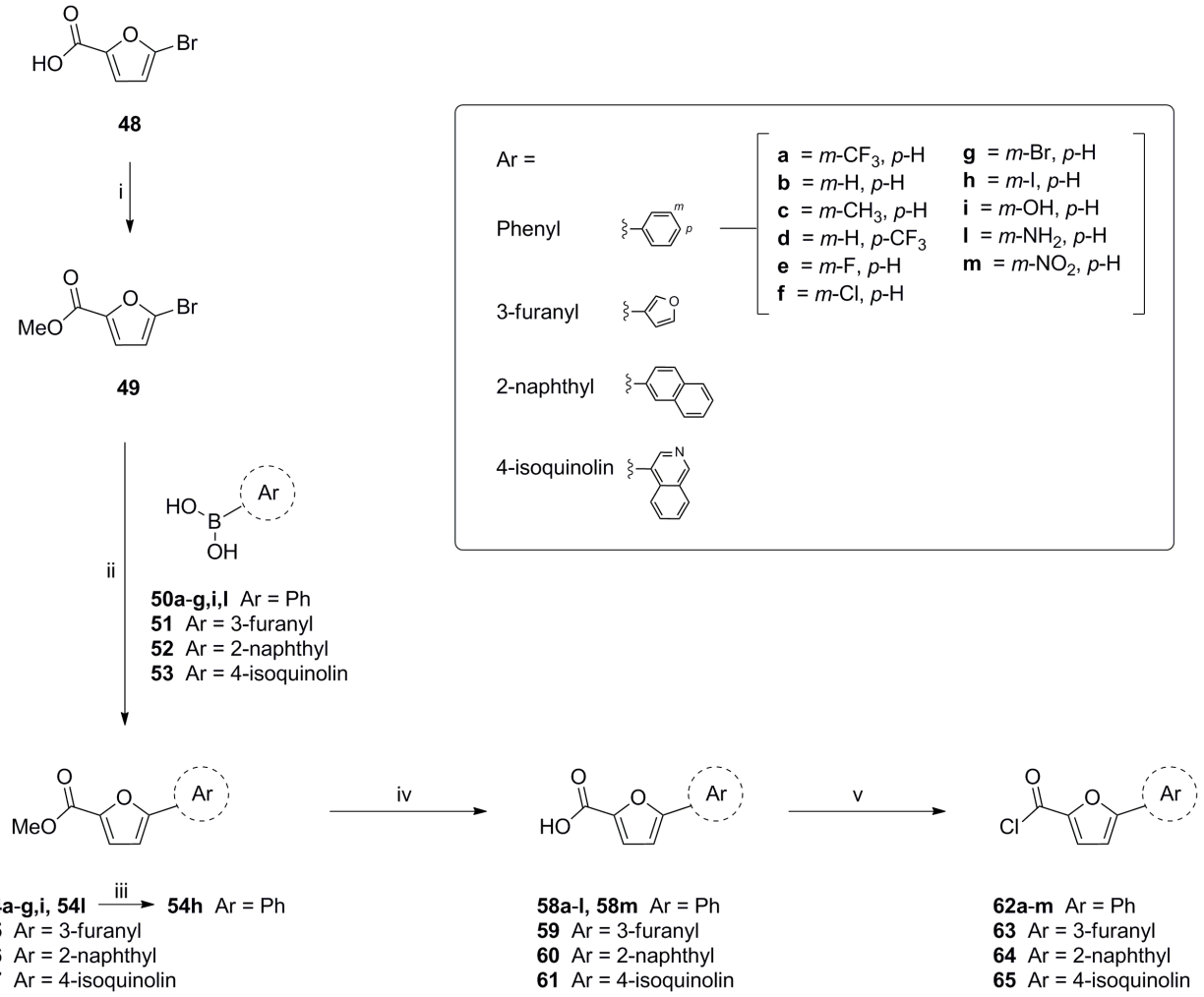


**Scheme 3.** Synthesis of carbonyl chlorides **62a-m** and **63-65**. Reagents and conditions: (i) conc $H_2SO_4$ (4 equiv), MeOH, reflux, overnight; (ii) $Pd(PPh_3)_4$ (0.05 equiv), $Na_2CO_3$ (4.2 equiv), anhydrous DME or DMF, reflux, 3–12 h; (iii) $NaNO_2$ (1.05 equiv), conc $H_2SO_4$ (0.2 mL/mmol), KI (1.5 equiv), water, 0 °C, 6 h; (iv) 1.5 M NaOH (1.5 equiv), THF, rt, overnight or 2.5 M LiOH (4 equiv), THF, rt, 48 h for **58i**; (v) $SOCl_2$ (23 equiv), 0 °C to reflux, 3–6 h.

NS6740 fragments **11-15** were prepared according to Scheme 4. The reaction between the carbonyl chloride intermediate **62a** and diethylamine in dichloromethane afforded the diethyl amide derivative **11**. Treatment of the 1,4-diazabicyclo[3.2.2]nonane dihydrochloride **16** with carbonyl chloride intermediate **62b**, the commercially available furan-2-carbonyl chloride **67** or acetyl chloride **68**, in the presence of cesium carbonate in dry dimethylformamide, provided compounds **12-14**. Subsequent reduction of **14** using lithium aluminum hydride in diethyl ether gave the *N*-ethyl diazabicyclic fragment **15**. The target compounds **12-15** were converted into their corresponding fumarates by treatment with fumaric acid in methanol.

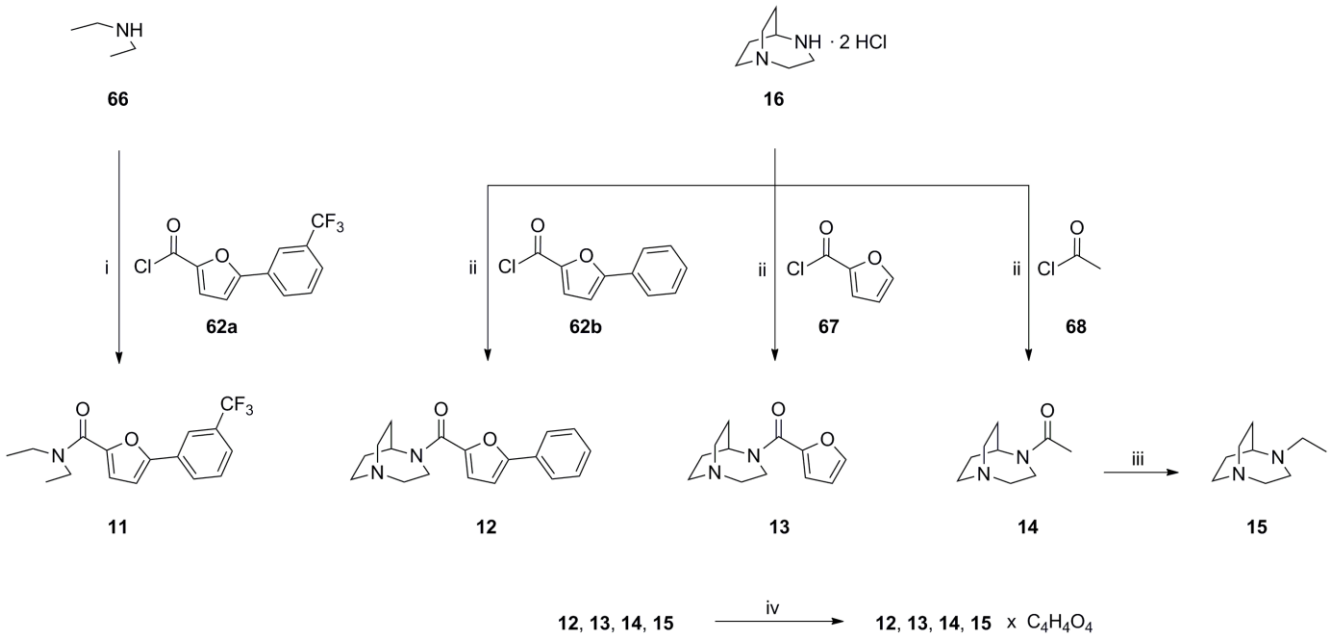


**Scheme 4.** Synthesis of NS6740 fragments **11**-**15**. Reagents and conditions: (i) anhydrous TEA (2 equiv), anhydrous $CH_2Cl_2$, rt, 1.5 h; (ii) $Cs_2CO_3$ (5 equiv), anhydrous DMF, 0 °C to rt, overnight; (iii) $LiAlH_4$ (2.25 equiv), anhydrous $Et_2O$, 0 °C to reflux, 3 h; (iv) fumaric acid (1 equiv), MeOH, rt, overnight.

The synthesis of NS6740 (**1**) and the analogs **17**-**20** is depicted in Scheme 5. The carbonyl chloride intermediate **62a** reacted with the diazabicyclic compound **16** to give **1**, which was converted into the corresponding methyl ammonium salt **17** by treatment with methyl iodide in methanol. The carbonyl group of **1** was reduced with lithium aluminum hydride in dry diethyl ether at reflux and yielded compound **20**. Compounds **18**, (*S*,*S*)-**19** and (*R*,*R*)-**19** were synthesized by acylation reaction of the carbonyl chloride **62a** with the 1,3-diazabicyclo[3.2.2]nonane dihydrochloride **37**, and the enantiomeric azabicyclic systems (*S*,*S*)-**43** and (*R*,*R*)-**43** respectively, under basic conditions at room temperature. The acylation step was followed by deprotection of the benzyl group by catalytic hydrogenation to give the enantiomers (*S*,*S*)-**19** and (*R*,*R*)-**19.** The free bases **1**, **18**, (*S*,*S*)-**19**, (*R*,*R*)-**19** and **20** were then treated with fumaric acid to provide the corresponding fumarates. Finally, NS6740 derivatives **21**-**32** were obtained by acylation reaction of the 1,4-diazabicyclo[3.2.2]nonane dihydrochloride **16** with the appropriate carbonyl chlorides **62c-m**, **63**-**65** under similar conditions as mentioned above. Again, we converted the analogues **21**-**32** into the corresponding fumarates by reaction with fumaric acid in methanol (Scheme 6).

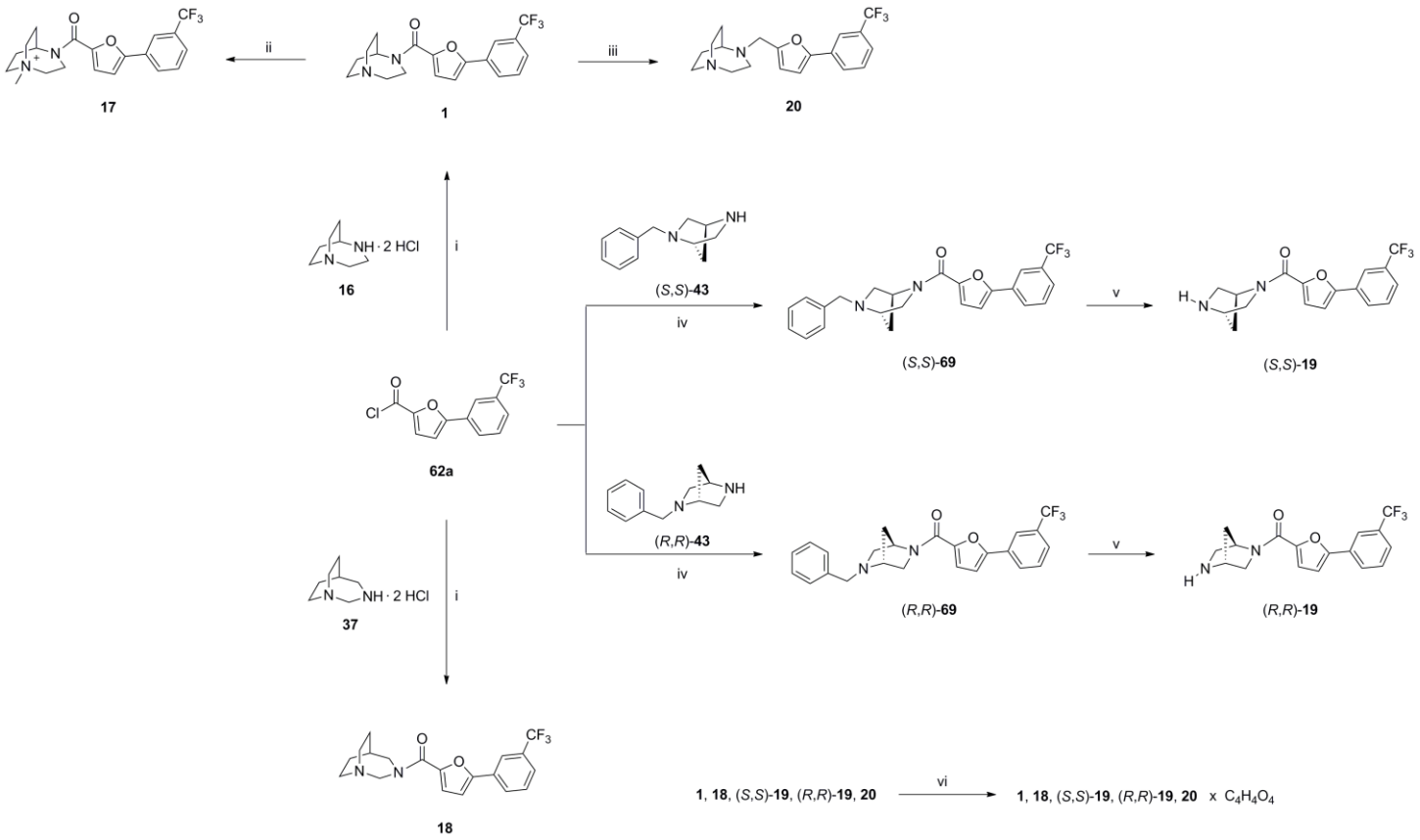


**Scheme 5.** Synthesis of NS6740 derivatives **17**, **18**, (*S*,*S*)-**19**, (*R*,*R*)-**19** and **20**. Reagents and conditions: (i) $Cs_2CO_3$ (5 equiv), anhydrous DMF, rt, overnight; (ii) MeI (8 equiv), MeOH, rt, overnight; (iii) $LiAlH_4$ (2.25 equiv), anhydrous $Et_2O$, 0 °C to reflux, 2 h; (iv) anhydrous TEA (1.1 equiv), anhydrous 1,4-dioxane, rt, 3 h; (v) $H_2$, Pd/C (10%), anhydrous MeOH, rt, overnight; (vi) fumaric acid (1 equiv), MeOH, rt, overnight.

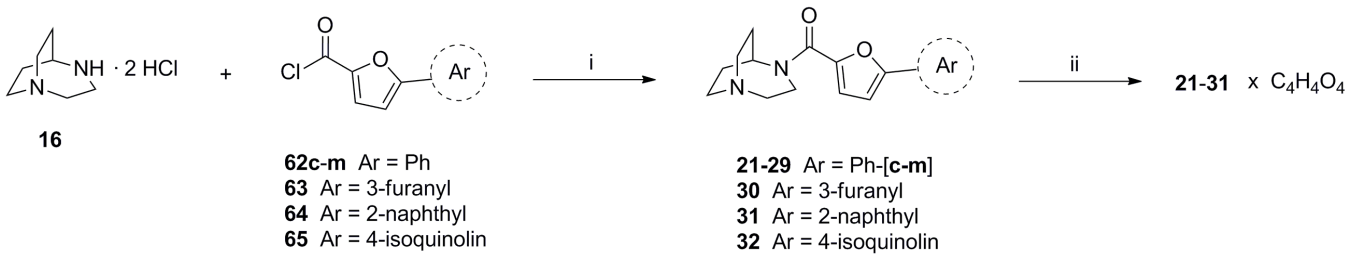


**Scheme 6.** Synthesis of NS6740 derivatives **21**–**32**. Reagents and conditions: (i) $Cs_2CO_3$ (5 equiv), anhydrous DMF, rt, overnight; (ii) fumaric acid (1 equiv), MeOH, rt, overnight. For structures **62c-m**, see Scheme 3, for structures **21-32**, see Fig. 2.

### *2.3. Electrophysiology*

The NS6740 fragments (**11**-**16**) and the new derivatives (**17**-**32**) were assayed on human α7 nAChRs expressed in *Xenopus laevis* oocytes with two-electrode voltage clamping [51]. The responses evoked at the α7 nAChR by the tested derivatives were measured both as peak-current and net-charge values at a holding potential of -60 mV. During drug applications at high concentrations, the α7 receptor currents were progressively more synchronized prior to the complete exchange of solution [52]. Therefore, to analyze and compare our results, we used net-charge values, which are less affected by channel synchronization than peak currents and have greater physiological relevance and scientific validity. Indeed, high levels of agonist binding site occupancy induce concentration-dependent desensitization of the α7 receptor subtype, which affects the relationship between peak current and net charge. For each derivative tested, the net-charge values represent the average of the responses from at least four different oocytes. For each oocyte, the test response was normalized to the average of two initial 60 μM ACh pre-controls (Fig. 3).

As previously described [26,36], NS6740 displays particularly prolonged receptor binding and a strong ability to stabilize the desensitized states of α7 nAChR. To analyze this electrophysiological profile of NS6740 and investigate the newly synthesized derivatives **11**-**32** as potential long-lasting desensitizers, we employed protocol I in which each compound was applied alone to evaluate its ability to promote channel opening. Then a 60 μM ACh post-control was delivered to verify the ability of the previously applied test drug to remain in the binding site and induce a prolonged desensitized state. Next there was an application of 10 μM of the type II PAM PNU-120596 to reveal the residual desensitized states induced by the test drug. Additionally, to highlight the induction of short-lasting desensitization, NS6740 and compounds **11**-**32** were investigated following protocol II in which the test drug was delivered in co-application with 10 μM of the type II PAM PNU-120596. Short-lasting silent agonists, in fact, do not cause either channel activation or prolonged desensitization when tested alone, but they give rise to channel potentiation only in co-application with PNU-120596. In Fig. 3 protocols I and II are illustrated for 10 μM applications of NS6740. Note that the colored bars above the applications in Fig. 3 serve as a key to the bar graphs in Fig. 4–7.

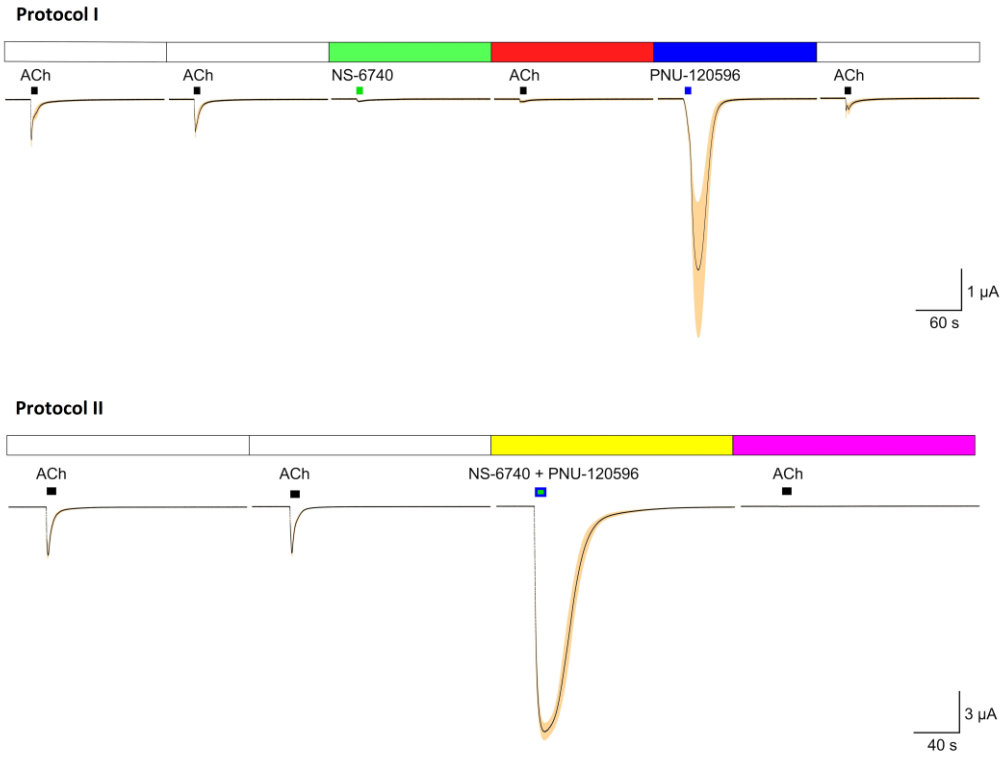


**Fig. 3.** Electrophysiological responses of NS6740 (**1**) at 10 μM. Data for each cell were normalized to the average of the peak-current amplitude of two initial 60 μM ACh controls. The solid lines are the averages, and the shaded areas are the standard error of the mean for each of the 10,322 data points. Each trace segment is 206.44 s long. Protocol I: cells ($n$ = 7) treated first with 10 μM NS6740 (green bar) and then with 60 μM ACh post-control (red bar), followed by 10 μM PNU-120596 (blue bar), and finally 60 μM ACh post-control. Protocol II: cells ($n$ = 5) treated first with 10 μM NS6740 plus 10 μM PNU-120596 (yellow bar), followed by 60 μM ACh post-control (purple bar).

The electrophysiological data of NS6740 (**1**) and compounds **11**-**32** are illustrated in Fig. 4–7 as net-charge responses, normalized to the average of the initial ACh controls on the vertical axis of the bar graphs. The ACh post-control net-charge responses of protocol II are not included in Fig. 5–7 since not relevant to the discussion. For both net-charge and peak-current values see Supplementary data, Table S1-S4.

Fig. 4 shows the electrophysiological results for NS6740 assayed at 1, 3, 10, and 30 μM. It displayed very weak partial agonist behavior at all four concentrations tested (Fig. 4A and Supplementary data, Table S1). Regarding the inhibition of the ACh response, a strong reduction of the post-control activity was displayed after application of NS6740 at 10 and 30 μM (net charges 0.19 ± 0.06 and 0.18 ± 0.04, respectively, Fig. 4B) due to the ability of the compound to promote deep receptor desensitization. Interestingly, the intensely potentiated response given by PNU-120596 alone was observed even after 3 μM NS6740 application (net charge 123.21 ± 71.01, 111.06 ± 37.18, and 57.41 ± 15.72, respectively at 3 μM, 10 μM, and 30 μM, Fig. 4C), thus revealing the prolonged residence time of NS6740 in the α7 receptor for drug concentrations ≥ 3 μM. Although 3 μM NS6740 showed a remarkable residual receptor potentiation by PNU-120596 (Fig. 4C), it did not provide a strong ACh post-control inhibition (Fig. 4B). Presumably only a

fraction of receptors are bound by the drug at low concentrations, or the drug may be bound at only a fraction of the sites. It may be that a lower fraction occupancy of the receptors is sufficient to generate a residual potentiated current due to prolonged receptor binding without affecting the ACh post-control response. The direct potentiated response obtained at 30 μM (net charge 2.73 ± 0.73, Fig. 4D) was much lower ($P$ = 0.0009) than the corresponding residual one (net charge 57.41 ± 15.72, Fig. 4C). This may be explained by the ability of higher concentrations of NS6740 to favor the faster stabilization of $D_i$ over $D_s$. Indeed, when the PAM was delivered few minutes after NS6740 in the first experiment (Fig. 4C), the α7 receptor had enough time to allow the transition from the $D_i$ to the $D_s$ state so that higher potentiation was observed. This confirmed what was previously described by Papke et al. [26]. Finally, the reduced ACh post-control response after co-application of 10 or 30 μM NS6740 with 10 μM PNU-120596 verified the sustained α7 receptor desensitization (Fig. 4E).

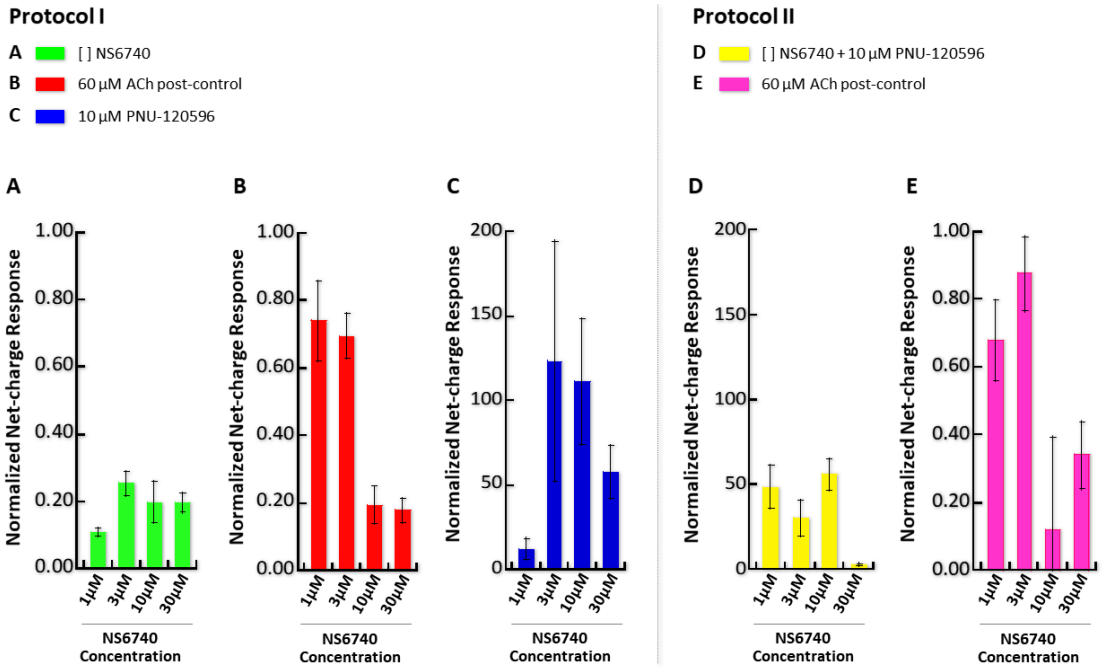


**Fig. 4.** Electrophysiological data of NS6740 (**1**) at 1, 3, 10, and 30 μM normalized to the average responses of the first two 60 μM ACh controls. Protocol I: (A) Direct activation by **1**; (B) 60 μM ACh post-control activation after the delivery of **1** indicating residual inhibition; (C) Residual potentiation by 10 μM PNU-120596 after the delivery of **1** and the 60 μM ACh post-control. Protocol II: (D) Direct potentiated response given by co-application of **1** plus 10 μM PNU-120596; (E) 60 μM ACh post-control activation.

The new NS6740 analogs **11-32** were analyzed at 10 μM following the previously described protocols I and II. The electrophysiological profiles of the NS6740 fragments **11-16** are illustrated in Fig. 5 (see also Supplementary data, Table S2). Fragment **11**, in which the basic nucleus was removed, and fragments **15** and **16**, in which only the basic nucleus was retained, proved to be completely inactive in terms of channel activation, ACh post-control inhibition, and receptor

potentiation (Fig. 5A–D). Derivative **12**, which lacks the *meta* trifluoromethyl group, showed increased partial agonist properties (net charge 0.54 ± 0.02, Fig. 5A) compared to the parent compound **1** (net charge 0.19 ± 0.06, brown bar) ($P$ = 0.0003). Interestingly, **12** was able to strongly inhibit the ACh post-control (net charge reduced to 0.14 ± 0.07, Fig. 5B) while producing a large residual potentiated response (net charge 18.33 ± 5.13, Fig. 5C), thus proving to be effective at inducing the $D_s$ state. Fragment **13**, without the phenyl moiety, displayed efficacious partial agonist behavior with a net charge of 0.71 ± 0.04 (≈ 70% of ACh response, Fig. 5A) and in co-application with PNU-120596 provided a direct PAM-potentiation (Fig. 5D) in line with what is expected for a partial agonist. The lack of residual potentiated response to PNU-120596 (Fig. 5C) by compound **13** indicated a failure to remain in the receptor long enough to stabilize a prolonged non-conductive state. Fragment **14**, retaining the carbonyl group and the diazabicyclic system, exhibited short-lasting silent agonist characteristics. Indeed, **14** did not give channel opening when tested alone (Fig. 5A) yet induced potentiation in co-application with PNU-120596 (Fig. 5D), thus proving its silent agonist behavior. The absence of the aromatic portion of the NS6740 pharmacophore resulted in a short-lasting interaction with the binding site that was evidenced by the full ACh post-control response (Fig. 5B) and by the lack of a residual PNU-120596-potentiated response (Fig. 5C).

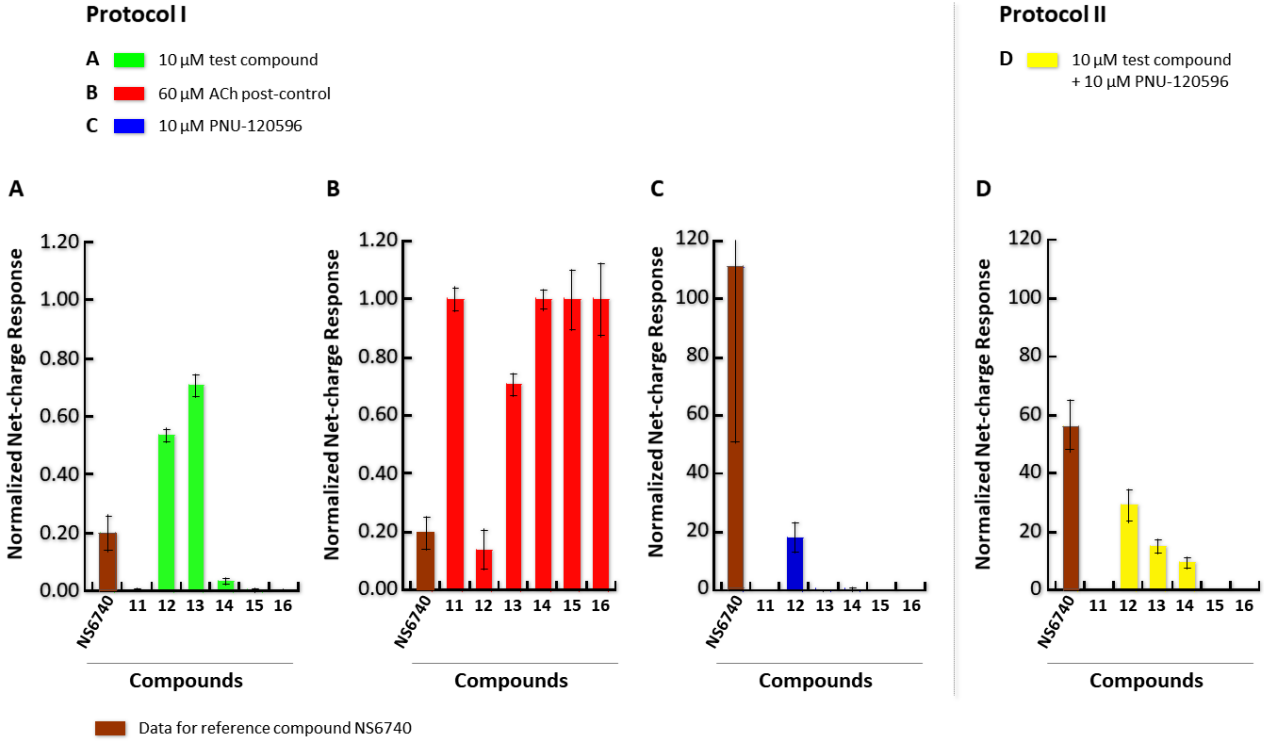


**Fig. 5.** Electrophysiological data of fragments **11-16** at 10 µM. Protocol I: (A) Channel opening given by **11-16**; (B) 60 µM ACh post-control activation after the delivery of **11-16**; (C) Residual potentiated response given by application of 10 µM PNU-120596 after delivery of **11-16** and the 60 µM ACh post-control. Protocol II: (D) Direct potentiated response given by **11-16** plus 10 µM PNU-120596.

The electrophysiological profiles of compounds **17-20** are reported in Fig. 6 (see also Supplementary data, Table S3). The methylammonium salt of NS6740 **17** displayed efficacious partial agonist behavior with a net charge of 0.79 ± 0.03 (≈ 80% of ACh response, Fig. 6A). It was not able to stabilize a prolonged non-conductive state and displayed a very small residual potentiated response (net charge 1.39 ± 0.86, Fig. 6C). Although the response was not strong, it induced a PAM-potentiation in line with what is expected for a partial agonist in co-application with PNU-120596 (Fig. 6D). In comparison with NS6740, compound **17** had an increased channel opening ability, a shorter residence time in the receptor binding site, and a reduced effectiveness in stabilizing the α7 desensitized state. The 1,3-diazabyciclo[3.2.2]nonane regioisomer of NS6740 **18** proved to be completely inactive in all the test conditions. The pair of enantiomers (*S*,*S*)-**19** and (*R*,*R*)-**19** exhibited large potentiated responses (15.22 ± 2.95 and 43.70 ± 3.30, respectively) in co-application with PNU-120596 (Fig. 6D). Given the absence of agonist responses (Fig. 6A) as well as of ACh post-control inhibitions and residual potentiations (Fig. 6B and Fig. 6C, respectively), we conclude that (*S*,*S*)-**19** and (*R*,*R*)-**19** behaved as silent agonists with readily reversible binding. The deletion of the carbonyl group (compound **20**) was detrimental to the activity, since this derivative behaved as a very weak partial agonist (Fig. 6A) without affecting the ACh post-control activity (red bar), and did not show any residual receptor PAM potentiation (Fig. 6C). Additionally, even in co-application with PNU-120596, **20** showed a negligible potentiation.

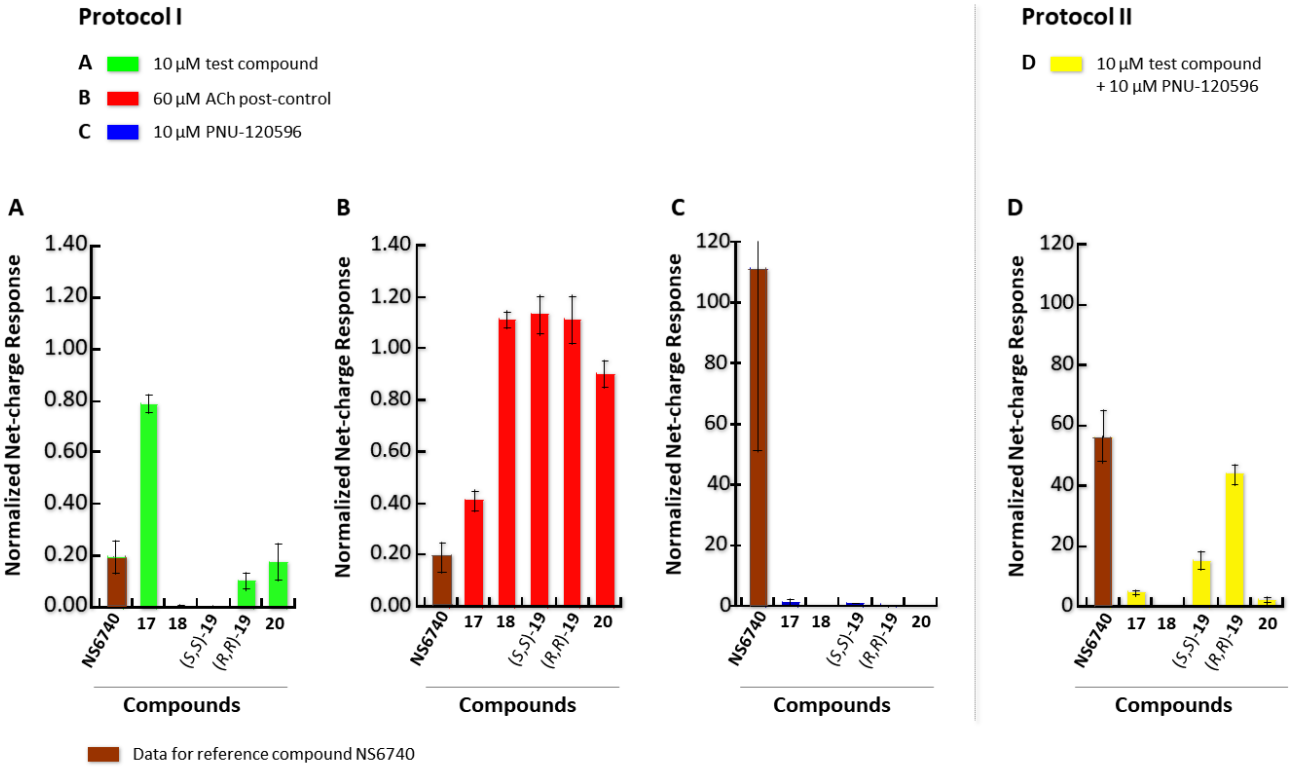


**Fig. 6.** Electrophysiological data of derivatives **17-20** at 10 µM. Protocol I: (A) Channel opening given by **17-20**; (B) 60 µM ACh post-control activation after the delivery of **17-20**; (C) Residual potentiated response given by application of 10 µM PNU-120596 after delivery of **17-20** and the 60 µM ACh post-control. Protocol II: (D) Direct potentiated response given by **17-20** plus 10 µM PNU-120596.

The profiles of compounds **21-32** at the α7 nAChR are summarized in Fig. 7 (see also Supplementary data, Table S4). Generally, the replacement of the original *meta* trifluoromethyl group on the aromatic ring conferred partial agonist activity to the new derivatives **21-32**, associated with a greater propensity of channel opening than the parent NS6740 (Fig. 7A), whereas both residual and direct PNU-120596-related responses were higher (Fig. 7C $0.0012 < P < 0.0445$ and Fig. 7D $0.00005 < P < 0.0101$, respectively) for the lead compound than for **21-32**. In detail, the *m*-methyl derivative **21** behaved as a weak partial agonist (Fig. 7A), displayed strong ACh post-control inhibition (net charge 0.20 ± 0.04, Fig. 7B), and a residual potentiated response (net charge 30.74 ± 8.77, Fig. 7C) higher ($P = 0.0283$) than the direct potentiation in co-application with PNU-120596 (Fig. 7D). Moving the trifluoromethyl group from the *meta* to *para* position (compound **22**) caused the loss of the peculiar NS6740 electrophysiological profile. **22** promoted more channel opening (net charge 0.40 ± 0.03, Fig. 7A), approximately 2-fold greater than that of the lead **1** (brown bar in Fig. 7A). Moreover, **22** did not show strong inhibition of ACh post-control (net charge 0.64 ± 0.06, Fig. 7B), with residual and direct potentiation (net charges 3.23 ± 0.65 and 6.25 ± 1.40, Fig. 7C and Fig. 7D, respectively) much lower than the parent compound **1**. The introduction of halogen atoms in the *meta* position of the phenyl ring, fluorine (**23**), chlorine (**24**), bromine (**25**), and iodine (**26**), gave weak partial agonist responses ranging from 25% to 50% of ACh control (Fig. 7A). Moreover, **23-26** showed strong ACh post-control inhibition, with almost total absence of the ACh response after the application of the chlorine-containing derivative **24** (net charge 0.04 ± 0.01, Fig. 7B). The large residual PAM-potentiated responses (Fig. 7C) suggested that halogen derivatives **23-26** induced prolonged α7 desensitization. Regarding the polar substituents, the *m*-hydroxy derivative **27** displayed weak partial agonist response (Fig. 7A), inhibition of ACh post-control (Fig. 7B), and remarkable residual PAM-potentiation (Fig. 7C). The *m*-amino compound **28** behaved as a typical short-lasting silent agonist, displaying very low agonist response (net charge 0.10 ± 0.02, Fig. 7A) and low ACh post-control inhibition (net charge 0.50 ± 0.04, Fig. 7B). Moreover, PAM potentiation was observed only in co-application with PNU-120596 (net charge 24.62 ± 3.30, Fig. 7D). Conversely, the nitro-containing derivative **29** behaved as a weak partial agonist with weak ACh post-control inhibition (Fig. 7A and Fig. 7B, respectively). The residual observed channel PNU-102596 potentiation was relatively low (net charge 4.78 ± 2.07, Fig. 7C), while the potentiation with co-application reflected what is expected for a partial agonist (net charge 12.19 ± 1.68, Fig. 7D). The furan derivative **30** acted as partial agonist with almost 50% of ACh response (Fig. 7A). The most interesting feature of **30** was its relatively long binding to the receptor, evidenced by considerable ACh post-control inhibition and large residual PAM-potentiated response (Fig. 7B and Fig. 7C, respectively). Regarding the bulkier naphthalene (**31**) and isoquinoline (**32**) derivatives, both displayed low agonist activity (net charges 0.15 ± 0.02 and 0.11 ± 0.02, respectively in Fig. 7A) and low ACh post-control inhibition

(net charges 1.18 ± 0.05 and 0.94 ± 0.03, respectively in Fig. 7B). Besides, the residual PNU-120596 potentiation (Fig. 7C) was completely absent. Surprisingly, in co-application with PNU-120596 (Fig. 7D), **31** did not show any direct potentiated response, while **32** gave a noticeable response (net charge 20.44 ± 11.77), which makes it a short-lasting silent agonist.

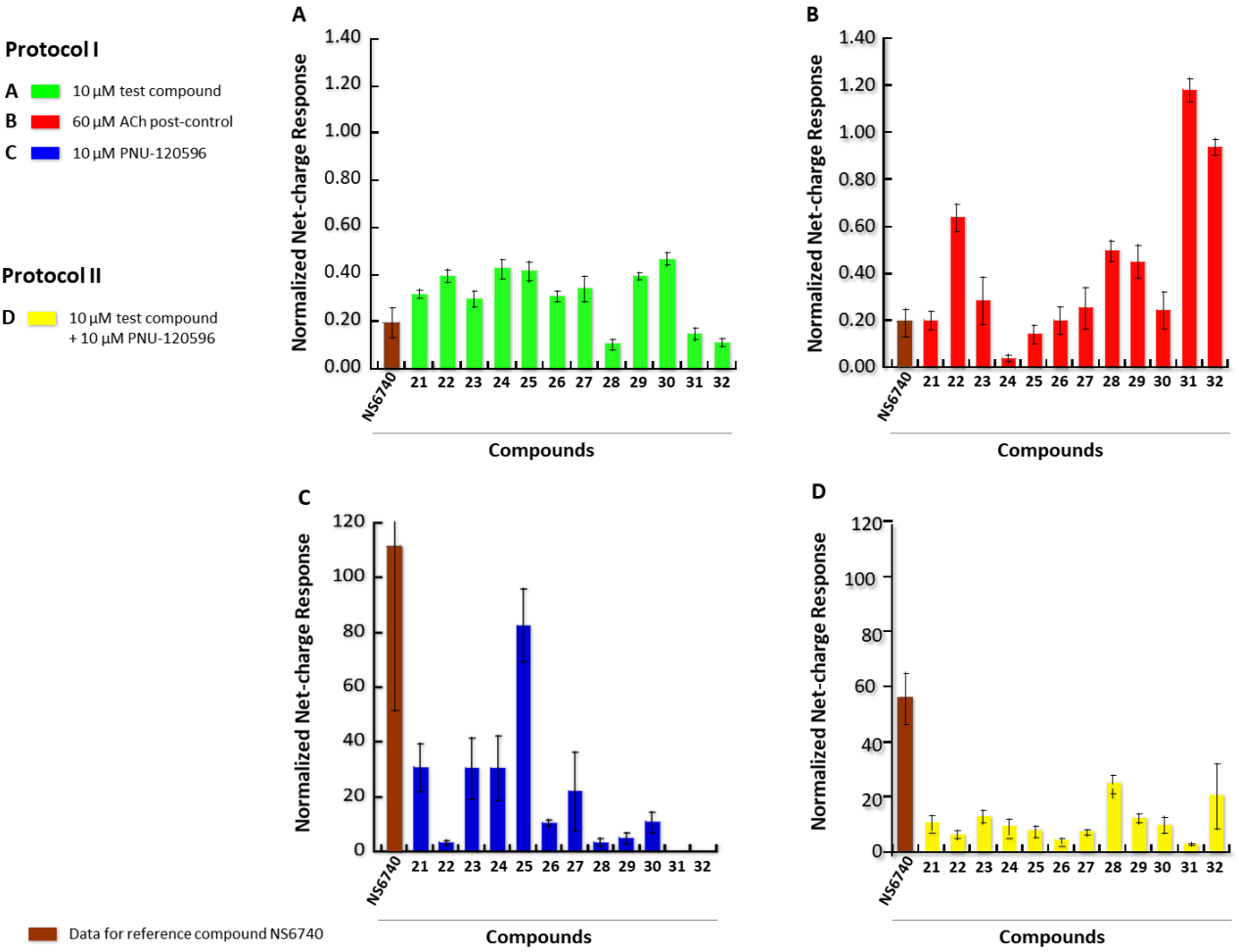


**Fig. 7.** Electrophysiological data of the NS6740 derivatives **21**-**32** at 10 µM. Protocol I: (A) Channel opening given by **21**-**32**; (B) 60 µM ACh post-control activation after the delivery of **21**-**32**; (C) Residual potentiated response given by application of type II PAM PNU-120596 after delivery of **21**-**32** and the 60 µM ACh post-control. Protocol II: (D) Direct potentiated response given by **21**-**32** plus 10 µM PNU-120596.

Among the studied compounds, fragment **13** and methylammonium derivative **17** behaved as efficacious partial agonists of the α7 nAChR, showing an increased ability to promote channel opening compared to **1** without inducing prolonged desensitized states. In particular, compounds **17** and **13** displayed comparable efficacy with $I_{max}$ values of 0.81 ± 0.01 and 0.71 ± 0.02, respectively, relative to 60 µM ACh. Compound **17** was twice as potent as

**13**, with $EC_{50}$ values of 322 ± 18 nM and 764 ± 52 nM, respectively. Concentration-response curves for **13** and **17** are provided in Fig. 8.

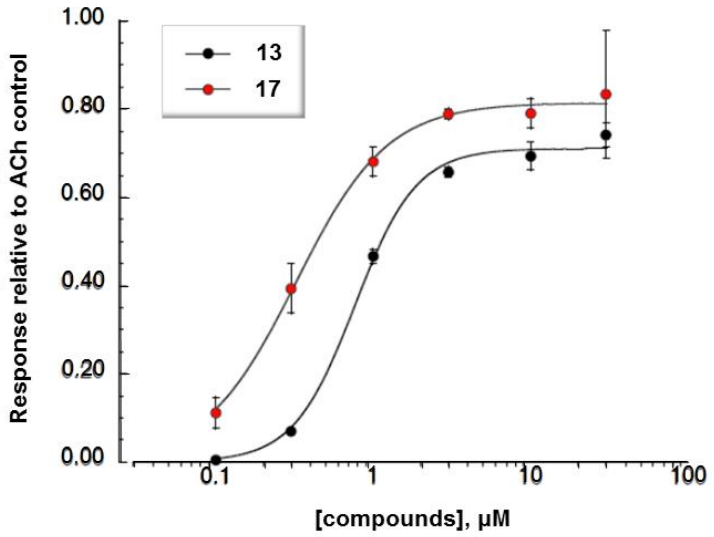


**Fig. 8.** Concentration-response curves for the α7 nAChR responses evoked by derivatives **13** and **17** at 0.1, 0.3, 1, 3, 10, and 30 μM measured as net charge. Data points represent the mean ± SEM from at least four oocytes and are normalized to 60 μM ACh control responses.

### *2.4. Structure-Activity Relationship (SAR) analyses of the synthesized compounds*

Electrophysiological assays were utilized to evaluate the activity profiles of the synthesized compounds (Fig. 2). The SAR analyses summarized in Fig. 9 focused on effects of the modifications of the lead compound NS6740 related to the three pharmacophoric regions, namely the positively charged diazabicyclic system, the central hydrogen-bond acceptor heterocyclic moiety, and the terminal phenyl group. The key features we are trying to pin down are low channel activation associated with prolonged receptor binding and stabilization of $D_s$ states. However, some derivatives are classifiable as partial agonists based on the greater efficacy in channel opening when applied alone, but they may also display an NS6740-like feature because of their ability to induce a sustained receptor desensitization. Initially, we investigated the effect of the NS6740 skeleton fragmentation (Fig. 2A). The focused series of six compounds **11-16** provided the first insight to the key moieties and functionalities that play important roles for inducing α7 silent activation. Removal of the basic diazabicyclic system with a residual diethylamide group in derivative **11** led to complete loss of activity. This result indicated that the interactions established by the protonatable nitrogen atom within the receptor binding site are essential for conferring to NS6740 its peculiar activity profile. When the trifluoromethyl group in *meta* position on the phenyl ring of **1** was removed, the resulting compound **12** appeared to be a partial agonist with desensitizing properties. This indicates the relevant role of this substituent in silencing the agonist

response, although it is not strictly required to stabilize the desensitized states. Interestingly, further removal of the phenyl group afforded compound **13**, which showed a very efficacious partial agonist activity, which is associated with a short-lasting receptor binding, thus proving the central role of the phenyl portion for inducing the desensitized states. The additional deletion of the furan ring further destabilized the receptor binding. Indeed, a short-lasting silent interaction was maintained as long as the carbonyl group was retained as a pharmacophore feature in compound **14**, while compounds **15** and **16** were completely devoid of activity, demonstrating that the diazabicyclic system as the positively charged center is an essential but not sufficient pharmacophoric feature for silent activation. On the whole, these results suggest that all the structural portions of NS6740 are required to confer its peculiar profile. In particular, the basic nucleus along with the hydrogen bond acceptor moiety and the aromatic moiety are associated with its ability to engender a strong desensitization. Additionally, the presence of the trifluoromethyl group seems to be related to the low channel opening that is typical of the very weak partial agonist **1**.

We next moved to exploring the distinct elements of the key scaffold (Fig. 2B). Concerning the 1,4-diazabicyclo[3.2.2]nonane system, the introduction of a permanent positive charge led to a strong partial agonist (compound **17**), although the desensitizing properties were compromised. Interestingly, the regioisomeric 1,3-diazabicyclo[3.2.2]nonane derivative **18** was completely inactive, demonstrating the critical role of the distance between the protonatable nitrogen atom and the carbonyl group to maintain a correct orientation in the binding domain for stimulating the receptor desensitization. Moreover, smaller dimensions of the basic nucleus and the introduction of a secondary amine (compounds (*S*,*S*)-**19** and (*R*,*R*)-**19**) gave a much shorter receptor binding duration.

Then we found that the deletion of the pharmacophoric carbonyl group (compound **20**) was detrimental to the α7 $D_s$ state. The loss of activity could be related to the absence of hydrogen bond interaction between the carbonyl group and the receptor, but also to different conformations that the more flexible derivative **20** may assume, as well for the presence of a second competitive protonatable center which may alter the interaction within the receptor binding site.

Finally, we examined the possible influences of substituents at the *meta* position of the phenyl moiety. Various groups with different sizes and electronic properties were used to replace the original trifluoromethyl group. In general, the introduction of different *meta* substituents determined an increase of partial agonist activity in terms of channel opening, whereas the PAM potentiation was differently affected depending on the substituent. The bioisosteric methyl group (compound **21**) as well as the halogen atoms (compounds **23**-**26**) and the hydroxyl group (compound **27**) maintained relevant desensitizing properties, while the introduction of the electron-withdrawing nitro group (compound **29**) and the electron-donor amino substituent

(compound **28**) shortened the permanence in the receptor binding pocket, suggesting different interactions established in the binding site. When we moved the original trifluoromethyl group from the *meta* to *para* position (compound **22**), we observed greater channel opening, which is associated with diminished stabilization of non-conducting receptor states. This could suggest a different orientation of the phenyl moiety in the receptor binding site. Finally, the phenyl moiety was replaced by different aromatic groups. Interestingly, the introduction of the furan ring in the place of the phenyl moiety (compound **30**) maintained a desensitizing profile, whereas the more hindered naphthyl- and isoquinoline-containing analogs (compounds **31** and **32**, respectively) did not preserve prolonged receptor binding and resulted in very weak partial agonists devoid of the ability to induce a sustained receptor desensitization. Therefore, we deduced that bulky substituents in the terminal aryl region are detrimental to establishing a stable receptor interaction. Fig. 9 summarizes the main structure–activity findings.

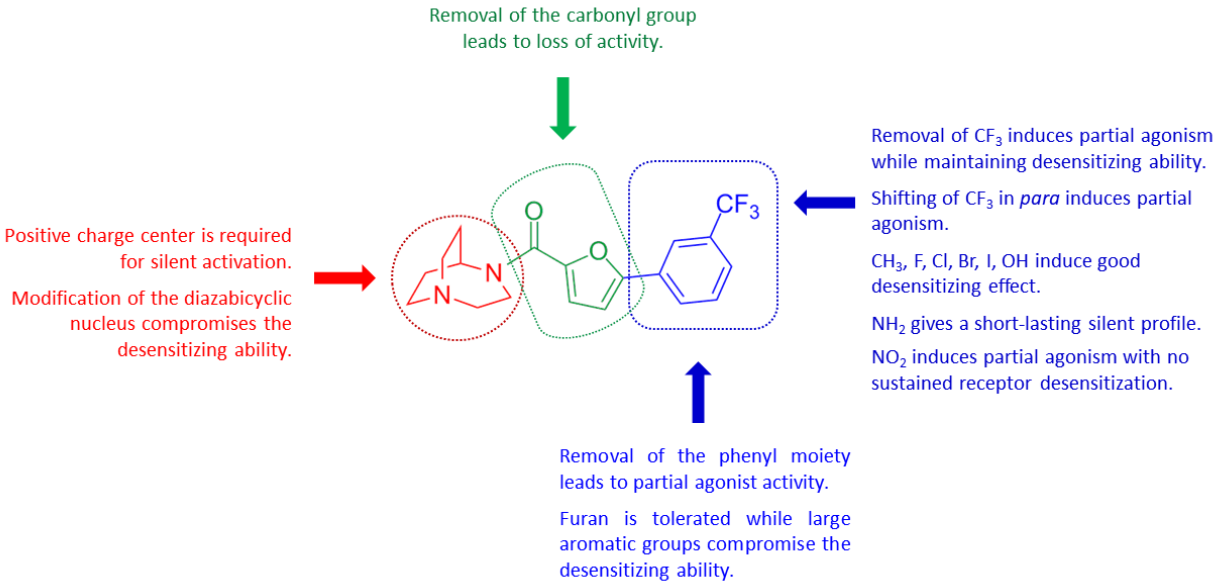


**Fig. 9.** Summary of the structure–activity relationships for the synthesized NS6740 derivatives.

## 3. Conclusion

In the present work, we extensively investigated the SARs of NS6740 (**1**), a very weak partial agonist able to promote strong α7 nAChR desensitization through induction of stable non-conducting states, which appear to be strictly related to the metabotropic activation mode of this receptor channel. The NS6740 skeleton was analyzed using a fragmentation approach and systematic molecular modifications performed at the main pharmacophore moieties, namely, the positively charged center, the hydrogen bond acceptor moiety, and the aromatic nucleus. Overall, the three relevant structural portions of NS6740 were found to be essential to the peculiar

electrophysiological behavior of this nicotinic ligand. Indeed, modifications of the basic nucleus led to loss of the NS6740 activity profile, and deletion of the central carbonyl group was detrimental to both the stabilization of the receptor binding and the subsequent sustained induction of receptor desensitization. The effects of the trifluoromethyl substituent on the phenyl ring were found to be critical in the *meta* more than in the *para* position. Moreover, insertion of halogen atoms and the methyl group in the *meta* position generally increased the partial agonist behavior. However, these ligands maintained prolonged receptor binding and sustained desensitization, whereas more polar groups produced a shorter residence time and a weaker stabilization of non-conducting states. Aromatic moieties bulkier than the phenyl ring decreased the binding stability, thus abolishing the prolonged stabilization of the receptor desensitization.

Among the new compounds, fragment **12**, *meta*-methyl **21** and *meta*-halogen derivatives **23-26**, and the furan analogue **30** emerged as novel α7 receptor desensitizers, overall displaying a partial agonist activity higher than that shown by **1**, but still associated with prolonged receptor binding and strong desensitization. Fragment **13** and methylammonium derivative **17** behaved also as efficacious partial agonists.

In summary, among the designed compounds, we identified a group of new promising desensitizing agents, which will be further studied to investigate the α7 metabotropic G-protein signaling and to evaluate their ability to modulate anti-inflammatory and analgesic responses. The results herein discussed reinforce the potential of a metabotropic activation of the α7 nAChR as an example of biased agonism for a receptor channel, whereby downstream activity is mediated by a mechanism other than the canonical channel opening. This may represent an approach for the treatment of pathological conditions such as inflammatory diseases and neuropathic pain.

## 4. Experimental Section

### *4.1. Chemistry*

All reagents and solvents were purchased from Sigma-Aldrich Srl (Milan, Italy) and were used without further purification. All reactions were carried out under inert atmosphere of argon or nitrogen and monitored by thin-layer chromatography (TLC) on commercial aluminum plates precoated with silica gel 60 (F-254, Merck) or with aluminum oxide (F-254, Fluka). Visualization was performed with UV light at 254 nm. Spots were further evidenced by spraying with a dilute alkaline potassium permanganate solution, or a phosphomolybdic acid solution, and with the Dragendorff reagent for tertiary amines and quaternary ammonium salts, or with an ethanolic solution of ninhydrin for aminoacids. Glassware was oven-dried or flame-dried prior to use. The synthesized compounds were purified on glass flash chromatography columns packed with silica gel (230–400 mesh particle size, pore size 60 Å, Merck). Melting points of solid products were measured in capillary tubes with a model B 540 Büchi apparatus and are uncorrected. Rotary power determinations (sodium D line, 589) were carried out with a Jasco P-1010 Polarimeter coupled with a Huber thermostat. $^{1}$H NMR and $^{13}$C NMR spectra were recorded with a Varian Mercury 300 ($^{1}$H, 300.063; $^{13}$C, 75.451 MHz) spectrometer at 20 °C. Abbreviations used for peak multiplicities are given as follows: s (singlet), br (broad signal), d (doublet), t (triplet), q (quartet), quint (quintet), m (multiplet), dd (doublet of doublets), td (triplet of doublets), qd (quartet of doublets), dt (doublet of triplets), ddt (doublet of doublet of triplets), ddd (doublet of doublets of doublets), qdd (quartet of doublets of doublets). Coupling constants (*J*) are given in Hz, chemical shifts ($\delta$) are expressed in parts per million (ppm) and calibrated for $^{1}$H using TMS and for $^{13}$C using residual deuterated solvent as internal standard ($CDCl_3$, 77.16 ppm; $CD_3OD$, 49.00 ppm; DMSO-$d_6$, 39.52 ppm; $(CD_3)_2CO$, 29.84 ± 0.01 ppm, 206.26 ± 0.13 ppm). The purity of compounds was determined to be over 95% (except for **20**, 92%) by UPLC–MS analysis performed on a Waters SYNAPTG2-Si system equipped with a Waters ACQUITY UPLC HSS T3 column, 1.8 μm, 2.1 mm × 100 mm. The injection volume of the sample was 10 μL, and the flow rate was 0.4 mL/min. The mobile phase consisted of 0.1 % formic acid in water (phase A), and acetonitrile (phase B). The time program elution was as follows: 0.0–1.0 min A/B 90:10, 1.0–3.0 min A/B 10:90, 3.0–7.0 min A/B 10:90, 7.0–7.1 min A/B 90:10, 7.2–10.0 min A/B 90:10 at 40 °C. For UV detection was used an ACQUITY PDA detector at 280 and 300 nm. For the high-resolution mass spectrometry (HRMS) measurements, electrospray ionization (ESI) mass spectra were obtained with a capillary voltage of 2.0 kV at a resolution of 40000–50000 units in positive-ion mode. Data are reported as mass-to-charge ratio (*m/z*) for the lead compounds **1** and the target compounds **11**-**32**.

The synthesis of intermediate compounds (*S*,*S*)-**43** and (*R*,*R*)-**43** (Scheme 2) and **62a−m**, **63**, **64**, **65 (**Scheme 3) is reported in the Supplementary Data.

### *4.1.1. Preparation of compounds **16** and **37***

#### *4.1.1.1. Quinuclidine-3-one oxime (**34**)*

To a stirred solution of hydroxylamine hydrochloride (16 g, 230.5 mmol, 1.15 equiv) and sodium acetate (48.4 g, 589.4 mmol, 3 equiv) in water (150 mL) was added dropwise quinuclidine-3-one hydrochloride **33** (32.4 g, 200.5 mmol, 1 equiv) dissolved in water (100 mL) and the reaction was heated at 70 °C for 2 h. The mixture was subsequently cooled to rt, and $Na_2CO_3$ was added portionwise, bringing the pH of the reaction mixture to 10. The resulting white precipitate was filtered off under reduced pressure and the aqueous layer was extracted with a mixture of $CH_2Cl_2$/*i*-PrOH 9:1 (3 × 200 mL). The organic layers were dried over anhydrous $Na_2SO_4$, filtered and concentrated under reduced pressure. Both the filtered and extracted solid residues were combined to afford **34** as a white amorphous solid (28 g, 100% yield); mp = 220–222 °C. $R_f$ = 0.43 ($CH_2Cl_2$/MeOH 4:1). $^1$H NMR (300 MHz, DMSO-$d_6$): $\delta$ 10.22 (s, 1H), 3.38 (s, 2H), 2.84–2.61 (m, 4H), 2.42 (quint, $J$ = 3.1 Hz, 1H), 1.78–1.56 (m, 4H). $^{13}$C NMR (75 MHz, DMSO-$d_6$): $\delta$ 162.21, 51.80, 46.73 (2C), 28.32, 26.38 (2C).

#### *4.1.1.2. Synthesis of **35** and **36***

The oxime intermediate **34** (38 g, 271.1 mmol) was added portionwise over 6 h to mechanically stirred polyphosphoric acid (95 mL) heated at 130 °C so as to obtain a light brown gummy mixture. The reaction was stirred at 130 °C overnight and the mixture's color changed to dark brown. The acidic mixture was then cooled to rt and ice-water (2 L) and 10 M NaOH were added to adjust the pH to 12−13. The aqueous phase was saturated with NaCl and extracted with a mixture of $CH_2Cl_2$/*i*-PrOH 4:1 (6 × 700 mL). The combined organic layers were dried over anhydrous $Na_2SO_4$, filtered, and concentrated under reduced pressure. The resulting crude was purified by silica gel column chromatography ($CH_2Cl_2$/MeOH 4:1) to afford the two regioisomers **35** as light brown amorphous solid (9.23 g, 24% yield) and **36** as light brown amorphous solid (1.64 g, 4.3% yield).

*4.1.1.2.1. 1,4-Diazabicyclo[3.2.2]nonan-3-one (**35**).* Mp = 211−213 °C. $R_f$ = 0.39 ($CH_2Cl_2$/MeOH 4:1). $^1$H NMR (300 MHz, $CDCl_3$): $\delta$ 6.91 (s, br 1H), 3.69 (s, 2H), 3.49–3.37 (m, 1H), 3.09 (qdd, $J$ = 14.5, 9.2, 5.6 Hz, 4H), 2.21–2.06 (m, 2H), 1.95-1.81 (m, 2H). $^{13}$C NMR (75 MHz, $CDCl_3$): $\delta$ 178.67, 62.30, 46.25 (2 C), 44.14, 30.20 (2 C).

*4.1.1.2.1. 1,3-Diazabicyclo[3.2.2]nonan-4-one (**36**).* Mp = 122−123 °C. $R_f$ = 0.41 ($CH_2Cl_2$/MeOH 95:5). $^1$H NMR (300 MHz, $CDCl_3$): $\delta$ 7.12 (br s, 1H), 5.82–5.72 (m, 1H), 5.70–5.61 (m, 1H), 3.12–3.02 (m, 5H), 2.70–2.61 (m, 2H), 2.24–2.13 (m, 2H). $^{13}$C NMR (75 MHz, $CDCl_3$): $\delta$ 173.95, 61.56, 52.91 (2C), 50.59, 26.28 (2C).

*4.1.1.3. 1,4-Diazabicyclo[3.2.2]nonane dihydrochloride (**16**)*

To a suspension of **35** (5.59 g, 39.9 mmol, 1 equiv) in anhydrous THF (70 mL) at 0 °C under an anhydrous and inert atmosphere was added dropwise a 1.0 M solution of $LiAlH_4$ in THF (47.9 mL, 47.9 mmol, 1.2 equiv). The mixture suspension was heated to refluxing temperature and a light-yellow solution was obtained. After refluxing for 8 h, the reaction was complete, and a white solid was crashed out. The excess of $LiAlH_4$ was quenched with EtOAc (50 mL) and few drops of MeOH at 0 °C, producing an additional white precipitate, which was removed by filtration. The yellow solution filtrate was subsequently treated with a 4.0 M solution of HCl in 1,4-dioxane (22.2 mL, 88.6 mmol, 2 equiv) and stirred at rt overnight. The corresponding hydrochloride salt **16** was obtained as a brown precipitate, which was isolated by vacuum filtration and recrystallized from MeOH/$Et_2O$ (4:1) to afford **16** as light brown prisms (4.2 g, 47.6% yield); mp = 307 °C (decomposed). $^1$H NMR (300 MHz, $CD_3OD$): $\delta$ 4.14 (quint, $J$ = 3.8 Hz, 1H), 3.81–3.73 (m, 2H), 3.68–3.42 (m, 6H), 2.40 (td, $J$ = 8.0, 3.8 Hz, 4H). $^{13}$C NMR (75 MHz, $CD_3OD$): $\delta$ 51.76, 49.22, 46.69 (2C), 38.77, 21.34 (2C). HRMS (ESI) $m/z$ calcd for $C_7H_{15}N_2$ 127.1235 $[M + H]^+$, found 127.1233.

*4.1.1.4. 1,3-Diazabicyclo[3.2.2]nonane dihydrochloride (**37**)*

This compound was prepared starting from the minor regioisomer **36** (700 mg, 4.99 mmol, 1 equiv) in anhydrous THF (9 mL) according to the method described for **16** to afford **37** as light brown prisms (600 mg, 45% yield); mp = 117−119 °C. $^1$H NMR (300 MHz, $CD_3OD$): $\delta$ 6.02 (d, $J$ = 10.4 Hz, 1H), 5.77 (d, $J$ = 10.4 Hz, 1H), 3.95–3.82 (m, 2H), 3.65–3.41 (m, 7H), 2.66–2.46(m, 2H). $^{13}$C NMR (75 MHz, $CD_3OD$): $\delta$ 53.70, 51.92, 50.86 (2C), 35.21, 23.43 (2C).

*4.1.2. Preparation of compounds **11−15***

*4.1.2.1. N,N-Diethyl-5-(3-(trifluoromethyl)phenyl)furan-2-carboxamide (**11**)*

To a solution of carbonyl chloride **62a** (515 mg 1.88 mmol, 1 equiv) in anhydrous $CH_2Cl_2$ (10 mL) was added dropwise at rt triethylamine (0.5 mL, 3.60 mmol, 2 equiv), followed by diethylamine **66** (0.19 mL, 1.88 mmol, 1 equiv). After stirring for 1.5 h at rt, the mixture was diluted with water (6 mL) and extracted with EtOAc (3 × 15 mL). The combined organic layers

were dried over anhydrous $Na_2SO_4$ and evaporated under reduced pressure. The crude residue was purified by silica gel column chromatography (cyclohexane/EtOAc 7:3) to afford the target compound **11** as a yellow solid (290 mg, 50% yield); mp = 45−48 °C. $R_f$ = 0.45 (cyclohexane/EtOAc 3:2). $^1$H NMR (300 MHz, $(CD_3)_2CO$): $\delta$ 8.11–8.05 (m, 2H), 7.76–7.66 (m, 2H), 7.20 (d, $J$ = 3.6 Hz, 1H), 7.11 (d, $J$ = 3.6 Hz, 1H), 3.77–3.45 (m, 4H), 1.48–1.15 (m, 6H). $^{13}$C NMR (75 MHz, $(CD_3)_2CO$): $\delta$ 159.29, 153.61, 149.91, 131.94, 131.75 (q, $J$ = 32.2 Hz), 130.94, 128.48, 125.45 (q, $J$ = 3.5 Hz), 125.10 (q, $J$ = 271.8 Hz), 121.39 (q, $J$ = 3.3 Hz), 118.29, 109.16, 42.61 (2C), 14.31 (2C). UPLC $t_R$ = 2.57 min; HRMS (ESI) $m/z$ calcd for $C_{16}H_{17}NO_2F_3$ 312.1211 $[M + H]^+$, found 312.1210.

*4.1.2.2. General procedure for the synthesis of **12−14***

To a stirred suspension of **16** (1 equiv) in anhydrous DMF (0.2 M) preheated at 60 °C for 40 min under inert atmosphere, $Cs_2CO_3$ (5 equiv) was added portionwise at rt to reach pH 8−9. The mixture was subsequently cooled down to 0 °C and the appropriate carbonyl chloride (1.2 equiv) was added portionwise. The reaction was then warmed to rt and stirred overnight. Upon completion, the mixture was diluted with water and extracted repeatedly with $CHCl_3$/*i*-PrOH (4:1). The combined organic layers were washed with brine (3 ×), dried over anhydrous $Na_2SO_4$, filtered and concentrated under vacuum to obtain compounds **12-14** as tertiary bases, which were converted to fumarate salts. The tertiary base (1 equiv) was dissolved in MeOH (0.2 M) and fumaric acid (1 equiv) was added. After stirring overnight at rt, the solvent was removed under reduced pressure and the crude salt was recrystallized from an appropriate solvent to give the desired final fumarate salts **12-14** × $C_4H_4O_4$.

*4.1.2.2.1. 1,4-Diazabicyclo[3.2.2]nonan-4-yl(5-phenylfuran-2-yl)methanone fumarate (**12**).* The title compound was prepared according to the general procedure from **16** (180 mg, 0.90 mmol, 1 equiv), $Cs_2CO_3$ (1.47 g, 4.52 mmol, 5 equiv), and carbonyl chloride **62b** (224 mg, 1.08 mmol, 1.2 equiv). After standard workup and subsequent reaction with fumaric acid (66 mg, 0.57 mmol, 1 equiv), the crude salt was recrystallized from MeOH to provide the pure fumarate salt **12** × $C_4H_4O_4$ as a white solid (180mg, 53% yield); mp = 174−176 °C. $^1$H NMR (300 MHz, $CD_3OD$): $\delta$ 7.82–7.75 (m, 2H), 7.49–7.33 (m, 3H), 7.22 (d, $J$ = 3.6 Hz, 1H), 6.97 (d, $J$ = 3.7 Hz, 1H), 6.71 (s, 2H), 4.91 (s, br 1H), 4.28 (s, br 2H), 3.59–3.44 (m, 6H), 2.48–2.13 (m, 4H). $^{13}$C NMR (75 MHz, $CD_3OD$): $\delta$ 170.45 (2C), 160.90, 157.61, 147.35, 135.89 (2C), 130.90, 130.08 (2C), 129.96, 125.56 (2C), 120.84, 107.90, 55.84, 47.14, 24.86. UPLC $t_R$ = 2.40 min; HRMS (ESI) $m/z$ calcd for $C_{18}H_{21}N_2O_2$ 297.1603 $[M + H]^+$, found 297.1609.

*4.1.2.2.2. 1,4-Diazabicyclo[3.2.2]nonan-4-yl(furan-2-yl)methanone fumarate (**13**).* The title compound was prepared according to the general procedure from **16** (180 mg, 0.90 mmol, 1 equiv), $Cs_2CO_3$ (1.47 g, 4.50 mmol, 5 equiv), and carbonyl chloride **67** (148 mg, 1.1 mmol, 0.11 mL, 1.2 equiv). After standard workup and subsequent reaction with fumaric acid (65 mg, 0.56 mmol, 1 equiv), the crude salt was recrystallized from MeOH/$Et_2O$ (4:1) to provide the pure fumarate salt **13** × $C_4H_4O_4$ as a white solid (100 mg, 53% yield); mp = 180−182 °C. $^1$H NMR (300 MHz, $CD_3OD$): $\delta$ 7.72 (dd, $J$ = 1.7, 0.7 Hz, 1H), 7.11 (d, $J$ = 3.4 Hz, 1H), 6.69 (s, 2H), 6.62 (dd, $J$ = 3.5, 1.8 Hz, 1H), 4.87–4.80 (m, 1H), 4.23 (s, br 2H), 3.52 (dt, $J$ = 15.9, 6.8 Hz, 6H), 2.42–2.10 (m, 4H). $^{13}$C NMR (75 MHz, $CD_3OD$): $\delta$ 171.27 (2C), 161.01, 148.34, 146.35, 136.10 (2C), 118.38, 112.63, 56.36, 46.96, 24.28. UPLC $t_R$ = 0.87 min; HRMS (ESI) $m/z$ calcd for $C_{12}H_{17}N_2O_2$ 221.1290 $[M + H]^+$, found 221.1288.

*4.1.2.2.3. 1-(1,4-Diazabicyclo[3.2.2]nonan-4-yl)ethanone fumarate (**14**).* The title compound was prepared according to the general procedure from **16** (150 mg, 0.75 mmol, 1 equiv), $Cs_2CO_3$ (1.20 g, 3.80 mmol, 5 equiv), and carbonyl chloride **68** (200 mg, 1.50 mmol, 0.06 mL, 1.2 equiv). After standard workup and subsequent reaction with fumaric acid (54 mg, 0.46 mmol, 1 equiv), the crude salt was recrystallized from EtOH/$Et_2O$ (4:1) to provide the pure fumarate salt **14** × 0.75 $C_4H_4O_4$ as a light brown solid (150 mg, 64% yield); mp = 169−170 °C. $^1$H NMR (300 MHz, $CD_3OD$): $\delta$ 6.68 (s, 1.5H), 4.80–4.71 (m, 0.5H), 4.46–4.37 (m, 0.5H), 4.06–3.97 (m, 1H), 3.96–3.87 (m, 1H), 3.52–3.37 (m, 6H), 2.20–2.10 (m, 4H), 2.15 (s, 3H). $^{13}$C NMR (75 MHz, $CD_3OD$): $\delta$ 171.86, 171.62 (2C), 136.21 (2C), 56.83, 55.90, 47.08, 46.82, 46.26, 30.67, 23.65, 22.03. HRMS (ESI) $m/z$ calcd for $C_9H_{17}N_2O$ 169.1341 $[M + H]^+$, found 169.1341.

*4.1.2.3. 4-Ethyl-1,4-diazabicyclo[3.2.2]nonane fumarate (**15**)*

To a suspension of **14** (300 mg, 1.78 mmol, 1 equiv) in anhydrous $Et_2O$ (14 mL) was added dropwise a suspension of $LiAlH_4$ (152 mg, 4 mmol, 2.25 equiv) in anhydrous $Et_2O$ (4 mL) at 0 °C under inert and anhydrous atmosphere. After refluxing for 3 h, the reaction was quenched with sodium sulfate decahydrate at 0 °C, the mixture was filtered, and the filtrate was concentrated under vacuum. The resulting residue compound **15** as free base (1 equiv) was reacted with fumaric acid (206 mg, 1.78 mmol, 1 equiv) at rt overnight. After evaporation of the solvent under reduced pressure, the crude salt was recrystallized from MeOH/$Et_2O$ (4:1) to provide the pure fumarate salt **15** × 2 $C_4H_4O_4$ as a white solid (165 mg, 25% yield); mp = 134−135 °C. $^1$H NMR (300 MHz, $CD_3OD$): $\delta$ 6.71 (s, 4H), 3.74–3.65 (m, 1H), 3.52–3.44 (m, 2H), 3.37–3.22 (m, 6H), 3.10 (q, $J$ = 7.2 Hz, 2H), 2.44–2.28 (m, 2H), 2.19–2.01 (m, 2H), 1.29 (t, $J$ = 7.2 Hz, 3H). $^{13}$C NMR (75 MHz, $CD_3OD$): $\delta$ 170.22 (2C), 135.82 (2C), 55.75, 52.30, 52.22, 47.44, 46.42 (2C), 21.94 (2C), 11.25. HRMS (ESI) $m/z$ calcd for $C_9H_{19}N_2$ 155.1548 $[M + H]^+$, found 155.1549.

*4.1.3. Preparation of compounds **1**, **17**, **18**, (S,S)-**19**, (R,R)-**19**, **20***

*4.1.3.1. 1,4-Diazabicyclo[3.2.2]nonan-4-yl(5-(3-trifluorophenyl)furan-2-yl)methanone fumarate (**1**)*

The title compound was prepared from **16** (425 mg, 2.13 mmol, 1 equiv), $Cs_2CO_3$ (3.48 g, 10.7 mmol, 5 equiv), and carbonyl chloride **62a** (703 mg, 2.56 mmol, 1.2 equiv) according to the general procedure described for compounds **12-14**. After standard workup, the free amine **1** was obtained as a yellow oil (404 mg, 52% yield), and was reacted with fumaric acid (76 mg, 0.66 mmol, 1 equiv) in MeOH. After evaporation of the solvent, the crude salt was recrystallized from EtOH to provide the pure fumarate salt **1** × $C_4H_4O_4$ as a white solid (100 mg, 30% yield); mp = 183−185 °C. $^1$H NMR (300 MHz, $CD_3OD$): $\delta$ 8.12–7.99 (m, 2H), 7.72–7.61 (m, 2H), 7.22 (d, $J$ = 3.6 Hz, 1H), 7.13 (d, $J$ = 3.7 Hz, 1H), 6.70 (s, 2H), 4.88 (s, br 1H), 4.28 (s, br 2H), 3.54 (dt, $J$ = 15.8, 7.6 Hz, 6H), 2.49–2.17 (m, 4H). $^{13}$C NMR (75 MHz, $CD_3OD$): $\delta$ 171.15 (2C), 160.78, 155.65, 147.96, 136.09 (2C), 132.50 (q, $J$ = 32.42 Hz), 131.85, 131.08, 129.00, 126.20 (q, $J$ = 3.46 Hz), 125.41 (q, $J$ = 271.78 Hz), 122.04 (q, $J$ = 3.46 Hz ), 120.36, 109.39, 56.02, 47.01, 24.02. UPLC $t_R$ = 3.00 min; HRMS (ESI) $m/z$ calcd for $C_{19}H_{20}N_2O_2F_3$ 365.1477 $[M + H]^+$, found 365.1475.

*4.1.3.2. 1-Methyl-4-(5-(3-(trifluoromethyl)phenyl)furan-2-carbonyl)-1,4-diazabicyclo[3.2.2]nonan-1-ium iodide (**17**)*

Methyl iodide (205 μL, 3.3 mmol, 8 equiv) was added dropwise to a solution of free base **1** (150 mg, 0.41 mmol, 1 equiv) in MeOH (5 mL). The mixture was stirred overnight at rt, then the solvent and excess methyl iodide were removed under reduced pressure. The resulting crude *N*-methylated analogue was recrystallized from *i*-PrOH and few drops of MeOH to provide the pure quaternary salt **17** as a white solid (85 mg, 40% yield); mp = 191−194 °C. $^1$H NMR (300 MHz, $CD_3OD$): $\delta$ 8.11–8.01 (m, 2H), 7.70–7.62 (m, 2H), 7.24 (d, $J$ = 3.7 Hz, 1H), 7.13 (d, $J$ = 3.6 Hz, 1H), 4.93 (s, br 1H), 4.36 (s, br 2H), 4.03–3.79 (m, 4H), 3.77–3.60 (m, 2H), 3.31 (s, 3H), 2.58–2.30 (m, 4H). $^{13}$C NMR (75 MHz, $CD_3OD$): $\delta$ 160.36, 155.78, 147.64, 132.44 ($J$ = 32 Hz), 131.76, 131.12, 129.10, 126.22 ($J$ = 3.4 Hz), 125.40 ($J$ = 271.50 Hz), 122.04 ($J$ = 3.4 Hz), 120.73, 109.47, 65.97, 58.54 (2C), 57.96, 47.44, 25.65 (2C). UPLC $t_R$ = 2.57 min; HRMS (ESI) $m/z$ calcd for $C_{20}H_{22}N_2O_2F_3$ 379.1633 $[M + H]^+$, found 379.1639.

*4.1.3.3. 1,3-Diazabicyclo[3.2.2]nonan-3-yl(5-(3-(trifluoromethyl)phenyl)furan-2-yl)methanone (**18**)*

The title compound was prepared from **37** (120 mg, 0.95 mmol, 1 equiv), $Cs_2CO_3$ (1.55 g, 4.75 mmol, 5 equiv), and carbonyl chloride **62a** (313 mg, 1.14 mmol, 1.2 equiv) according to the

general procedure described for compounds **12**-**14**. After standard workup and subsequent reaction with fumaric acid (50 mg, 0.43 mmol, 1 equiv), the crude salt was recrystallized from EtOH/$Et_2O$ (4:1) to provide the pure fumarate salt **18** × $C_4H_4O_4$ as a light brown solid (105 mg, 50% yield); mp = 122−124 °C. $^1$H NMR (300 MHz, $CD_3OD$): $\delta$ 8.24–8.18 (m, 1H), 8.16–8.07 (m, 1H), 7.72–7.62 (m 2H), 7.28 (d, $J$ = 3.6 Hz, 1H), 7.12 (d, $J$ = 3.6 Hz, 1H), 6.68 (s, 2H), 5.99 (d, $J$ = 10.5 Hz, 1H), 5.77 (d, $J$ = 10.6 Hz, 1H), 3.90–3.71 (m, 4H), 3.46–3.32 (m, 5H), 2.54–2.41 (m, 2H). $^{13}$C NMR (75 MHz, $CD_3OD$): $\delta$ 170.92 (2C), 161.43, 155.87, 148.30, 136.04 (2C), 132.50 (q, $J$ = 32.2 Hz), 130.93, 129.16, 126.58, 126.17 (q, $J$ = 3.5 Hz), 125.48 (q, $J$ = 270.6 Hz), 122.16 (q, $J$ = 3.8 Hz), 117.97, 109.78, 57.06, 51.98, 50.45 (2C), 35.59, 23.85 (2C). UPLC $t_R$ = 2.65 min; HRMS (ESI) $m/z$ calcd for $C_{19}H_{20}N_2O_2F_3$ 365.1477 $[M + H]^+$, found 365.1480.

#### *4.1.3.4. Synthesis of intermediates (S,S)-**69** and (R,R)-**69***

##### *4.1.3.4.1. (1S,4S)-5-Benzyl-2,5-diazabicyclo[2.2.1]heptan-2-yl)(5-(3-(trifluoromethyl)phenyl)furan-2-yl)methanone ((S,S)-**69**)*

To a solution of (*S*,*S*)-**43** (206 mg, 0.59 mmol, 1 equiv) in anhydrous 1,4-dioxane (15 mL) was added anhydrous triethylamine (0.09 mL, 0.65 mmol, 1.1 equiv) at 0 °C under anhydrous atmosphere. After stirring for 10 min, carbonyl chloride **62a** (162 mg, 0.59 mmol, 1 equiv) in 1,4-dioxane (10 mL) was added dropwise and the mixture was then warmed at rt. Upon completion (3 h), the formed precipitate was removed by filtration and the filtrate was evaporated under vacuum. The resulting crude residue was repeatedly treated with cyclohexane/EtOAc (1:1). The combined organic layers were evaporated under reduced pressure to afford (*S*,*S*)-**69** as a pale yellow oil (450 mg, 96% yield). $R_f$ = 0.39 (cyclohexane/EtOAc 3:2). $[\alpha]^{20}_D$ = +11.0 (c = 1.05, $CHCl_3$). $^1$H NMR (300 MHz, $CDCl_3$): $\delta$ 7.85–7.62 (m, 2H), 7.52–7.35 (m, 2H), 7.34–7.04 (m, 6H), 6.78–6.67 (m, 1H), 5.09–4.96 (m, 0.5 H), 4.93–4.80 (0.5H), 4.13–3.99 (m, 0.5H) 3.88–3.62 (m, 2.5H), 3.61–3.36 (m, 2H), 3.18–3.05 (m, 0.5H), 2.93–2.72 (m, 1.5H), 2.06–1.84 (m, 1H), 1.82–1.62 (m, 1H). $^{13}$C NMR (75 MHz, $CDCl_3$): $\delta$ 157.30, 154.03, 148.57, 139.00, 131.61 (q, $J$ = 31.7 Hz), 130.76, 129.78, 129.62 (2C), 128.58 (2C), 127.52, 127.33, 125.06 (q, $J$ = 3.8 Hz), 125.62 (q, $J$ = 271.5 Hz), 121.15 (q, $J$ = 3.5 Hz), 118.51, 108.09, 61.13, 59.73, 58.98, 57.66, 53.16, 35.45.

##### *4.1.3.4.2. (1R,4R)-5-Benzyl-2,5-diazabicyclo[2.2.1]heptan-2-yl)(5-(3-(trifluoromethyl)phenyl)furan-2-yl)methanone ((R,R)-**69**)*

The title compound was prepared as described for (*S*,*S*)-**69** starting from (*R*,*R*)-**43** (120 mg, 0.64 mmol, 1 equiv), anhydrous triethylamine (0.07 mL, 0.70 mmol, 1.10 equiv), and carbonyl chloride **62a** (175 mg, 0.64 mmol, 1 equiv) to afford (*R*,*R*)-**69** as a yellow oil (220 mg, 81% yield). $R_f$ = 0.39 (cyclohexane/EtOAc 3:2). $[\alpha]^{20}_D$ = −11.0 (*c* 1.05, $CHCl_3$). $^1$H NMR (300 MHz, $CD_3OD$): $\delta$

8.13–7.95 (m, 2H), 7.71–7.60 (m, 2H), 7.46–7.17 (m, 6H), 7.15–7.08 (m, 1H), 5.20–5.13 (m, 0.5H), 4.93–4.87 (m, 0.5H), 4.18–4.08 (m, 0.5H), 3.95–3.87 (m, 0.5H), 3.86–3.80 (m, 2H), 3.69–3.75 (m, 1.5H), 3.57–3.49 (m, 0.5H), 3.20–3.12 (m, 0.5H), 3.01–2.82 (m, 1.5H), 2.15–2.01 (m, 1H), 1.96–1.81 (m, 1H). $^{13}$C NMR (75 MHz, $CD_3OD$): $\delta$ 159.10, 155.86, 148.63, 139.64, 132.52 (q, $J$ = 32.4 Hz), 131.93, 131.06, 129.99 (2C), 129.51 (2C), 129.03, 128.41, 126.14 (q, $J$ = 3.7 Hz), 125.42 (q, $J$ = 271.5 Hz), 122.08 (q, $J$ = 4.1 Hz), 119.85, 109.52, 62.54, 60.41, 59.87, 59.12, 54.60, 34.48.

*4.1.3.5. Synthesis of (S,S)-**19** and (R,R)-**19***

*4.1.3.5.1. (1S,4S)-2,5-Diazabicyclo[2.2.1]heptan-2-yl(5-(3-(trifluoromethyl)phenyl)furan-2-yl)methanone fumarate ((S,S)-**19**).*

To a solution of (*S*,*S*)-**69** (300 mg, 0.7 mmol, 1 equiv) in anhydrous MeOH (12 mL) was added 10% Pd/C (30 mg). After being stirred overnight at rt under $H_2$ atmosphere, the reaction mixture was filtered through a Celite pad and evaporated under vacuum. The residue was reacted with fumaric acid (69 mg, 0.59 mmol, 1 equiv) in MeOH (6 mL). After evaporation of the solvent under reduced pressure, the crude salt was recrystallized from EtOH/*i*-PrOH/$Et_2O$ (4:2:1) to provide the pure fumarate salt (*S*,*S*)-**19** × 0.5 $C_4H_4O_4$ as a white solid (15 mg, 9% yield); mp = 120−121 °C. $[\alpha]^{20}_D$ = +24.0 (*c* 1.1, MeOH). $^1$H NMR (300 MHz, $CD_3OD$): $\delta$ 8.10–7.97 (m, 2H), 7.72–7.59 (m, 2H), 7.30 (d, $J$ = 3.5 Hz, 1H), 7.13 (d, $J$ = 3.4 Hz, 1H), 6.64 (s, 1H), 5.53–5.39 (m, 0.2H), 5.18–5.01 (m, 0.8H), 4.66–4.38 (m, 1H), 4.31–4.08 (m, 1H), 3.91–3.67 (m, 1H), 3.66–3.35 (m, 2H), 2.32–1.95 (m, 2H). $^{13}$C NMR (75 MHz, $CD_3OD$): $\delta$ 172.83 (2C), 159.28, 156.15, 148.18, 136.57 (2C), 132.52 (q, $J$ = 32.0 Hz), 131.75, 131.13, 129.05, 126.31 (q, $J$ = 3.4 Hz), 125.38 (q, $J$ = 270.1 Hz), 122.11 (q, $J$ = 3.4 Hz), 120.47, 109.69, 59.47, 56.74, 53.91, 52.77, 35.60. UPLC $t_R$ = 2.56 min; HRMS (ESI) $m/z$ calcd for $C_{17}H_{16}N_2O_2F_3$ 337.1164 $[M + H]^+$, found 337.1165.

*4.1.3.5.2. (1R,4R)-2,5-Diazabicyclo[2.2.1]heptan-2-yl(5-(3-(trifluoromethyl)phenyl)furan-2-yl)methanone fumarate ((R,R)-**19**).*

The title compound was prepared as described for (*S*,*S*)-**19** starting from (*R*,*R*)-**69** (140 mg, 0.32 mmol, 1 equiv). After standard workup and subsequent reaction with fumaric acid (69 mg, 0.59 mmol, 1 equiv) in MeOH, the crude salt was recrystallized from EtOH/*i*-PrOH/$Et_2O$ (4:2:1) to provide the pure fumarate salt (*R*,*R*)-**19** × 0.5 $C_4H_4O_4$ as a white solid (11 mg, 10% yield); mp = 119−120 °C. $[\alpha]^{20}_D$ = −24.3 (*c* 1.05, MeOH). $^1$H NMR (300 MHz, $CD_3OD$): $\delta$ 8.13–7.95 (m, 2H), 7.75–7.57 (m, 2H), 7.30 (d, $J$ = 3.5 Hz, 1H), 7.14 (d, $J$ = 3.5 Hz, 1H), 6.65 (s, 1H), 5.54–5.29 (m, 0.2H), 5.20–4.97 (m, 0.8H), 4.62–4.39 (m, 1H), 4.29–4.06 (m, 1H), 3.89–3.67 (m, 1H), 3.65–3.35 (m, 2H), 2.30–1.96 (m, 2H). $^{13}$C NMR (75 MHz, $CD_3OD$): $\delta$ 172.79 (2C), 159.30, 156.16, 148.20,

136.56 (2C), 132.53 (q, *J* = 32.1 Hz), 131.76, 131.13, 129.06, 126.32 (q, *J* = 3.4 Hz), 125.39 (q, *J* = 270.0 Hz), 122.11 (q, *J* = 3.4 Hz), 120.43, 109.69, 59.46, 56.74, 53.97, 52.78, 35.62. UPLC $t_R$ = 2.53 min; HRMS (ESI) *m*/*z* calcd for $C_{17}H_{16}N_2O_2F_3$ 337.1164 $[M + H]^+$, found 337.1165.

*4.1.3.6. 4-((5-(3-(Trifluoromethyl)phenyl)furan-2-yl)methyl)-1,4 diazabicyclo[3.2.2]nonane fumarate (**20**).*

To a solution of **1** (170 mg, 0.47 mmol, 1 equiv) in anhydrous $Et_2O$ (4 mL) was added dropwise a suspension of $LiAlH_4$ (39.8 mg, 1.05 mmol, 2.25 equiv) in anhydrous $Et_2O$ (1 mL) at 0 °C under anhydrous atmosphere. After stirring at reflux for 2 h, the reaction was cooled at 0 °C and quenched with a saturated aqueous solution of sodium tartrate, and then the mixture was extracted with $CH_2Cl_2$ (3 × 4 mL). The pooled organic layers were dried over anhydrous $Na_2SO_4$, filtered, and concentrated under vacuum. The resulting residue compound **20** as free base (1 equiv) was reacted with fumaric acid (27 mg, 0.23 mmol) in MeOH at rt overnight. After evaporation of the solvent under reduced pressure, the crude salt was recrystallized from EtOH/$Et_2O$ (4:1) to provide the pure fumarate salt **20** × 2 $C_4H_4O_4$ as a white solid (30 mg, 11% yield); mp = 106−108 °C. $^1$H NMR (300 MHz, $CD_3OD$): $\delta$ 8.22–8.12 (m, 2H), 7.86–7.72 (m, 2H), 7.13 (d, *J* = 3.3 Hz, 1H), 6.95 (s, 4H), 6.72 (d, *J* = 3.3 Hz, 1H), 4.13 (s, 2H), 3.75–3.51 (m, 9H), 2.50–2.32 (m, 2H), 2.30–2.13 (m, 2H). $^{13}$C NMR (75 MHz, $CD_3OD$): $\delta$ 169.86 (2C), 153.72, 153.47, 135.72 (2C), 132.97, 132.27 (q, *J* = 32.1 Hz), 130.76, 128.02, 125.56 (q, *J* = 271.7 Hz), 124.75 (q, *J* = 4.0 Hz), 120.91 (q, *J* = 4.0 Hz), 112.69, 108.61, 54.86, 54.05, 52.85, 47.47 (2C), 46.64, 22.91 (2C). UPLC $t_R$ = 2.56 min; HRMS (ESI) *m*/*z* calcd for $C_{19}H_{22}N_2OF_3$ 351.1684 $[M + H]^+$, found 351.1678.

*4.1.4. Preparation of compounds **21−32***

The title compounds were prepared following the general procedure described for the preparation of compounds **12−14** from the 1,4-diazabicyclo[3.2.2]nonane dihydrochloride **16** (1 equiv), $Cs_2CO_3$ (5 equiv), and the appropriate carbonyl chloride (**62c**−**m**, **63**, **64**, **65**) (1.2 equiv). After standard workup, subsequent reaction of the free base (except for **32** isolated as free base) with fumaric acid (1 equiv) in MeOH and recrystallization of the crude salt from an appropriate solvent afforded the desired final fumarate salts **21**-**31** × $C_4H_4O_4$.

*4.1.4.1. 1,4-Diazabicyclo[3.2.2]nonan-4-yl(5-(m-tolyl)furan-2-yl)methanone fumarate (**21**).* The title compound was prepared according to the general procedure from **16** (150 mg, 0.75 mmol, 1 equiv), $Cs_2CO_3$ (1.23 g, 3.77 mmol, 5 equiv), and carbonyl chloride **62c** (200 mg, 1.50 mmol, 1.2 equiv). After standard workup and subsequent reaction with fumaric acid (59 mg, 0.50 mmol, 1 equiv), the crude salt was recrystallized from EtOH/$Et_2O$ (4:1) to provide the pure fumarate salt **21** × $C_4H_4O_4$ as a brown solid (150 mg, 64% yield); mp = 157−159 °C. $^1$H NMR (300 MHz,

$CD_3OD$): $\delta$ 7.63–7.51 (m, 2H), 7.32 (t, $J$ = 7.6 Hz, 1H), 7.23–7.15 (m, 2H), 6.93 (d, $J$ = 3.6 Hz, 1H), 6.70 (s, 2H), 4.91 (s, br 1H), 4.28 (s, br 2H), 3.54 (dt, $J$ = 15.5, 6.9 Hz, 6H), 2.48–2.16 (m, 4H), 2.39 (s, 3H). $^{13}$C NMR (75 MHz, $CD_3OD$): $\delta$ 171.12 (2C), 160.91, 157.77, 147.19, 139.98, 136.07 (2C), 130.82, 130.70, 129.99, 126.06, 122.74, 120.84, 107.78, 55.72, 47.03, 24.52, 21.45. UPLC $t_R$ = 2.51 min; HRMS (ESI) $m/z$ calcd for $C_{19}H_{23}N_2O_2$ 311.1760 $[M + H]^+$, found 311.1757.

*4.1.4.2. 1,4-Diazabicyclo[3.2.2]nonan-4-yl(5-(4-trifluorophenyl)furan-2-yl)methanone fumarate (**22**).* The title compound was prepared according to the general procedure from **16** (105 mg, 0.53 mmol, 1 equiv), $Cs_2CO_3$ (865 mg, 2.65 mmol, 5 equiv), and carbonyl chloride **62d** (175 mg, 0.64 mmol, 1.2 equiv). After standard workup and subsequent reaction with fumaric acid (48 mg, 0.41 mmol, 1 equiv), the crude salt was recrystallized from EtOH to provide the pure fumarate salt **22** × 1.5 $C_4H_4O_4$ as an off-white solid (100 mg, 50% yield); mp = 167−169 °C. $^1$H NMR (300 MHz, $CD_3OD$): $\delta$ 7.98 (d, $J$ = 8.3 Hz, 2H), 7.75 (d, $J$ = 8.4 Hz, 2H), 7.24 (d, $J$ = 3.6 Hz, 1H), 7.14 (d, $J$ = 3.7 Hz, 1H), 6.71 (s, 3H), 4.90 (s, br 1H), 4.32 (s, br 2H), 3.66–3.46 (m, 6H), 2.51–2.16 (m, 4H). $^{13}$C NMR (75 MHz, $CD_3OD$): $\delta$ 170.27 (2C), 160.69, 155.68, 148.25, 135.83 (2C), 134.34, 131.26 (q, $J$ = 32.8 Hz), 127.03 (2C) (q, $J$ = 3.7 Hz), 125.95 (2C), 125.50 (q, $J$ = 271.1 Hz), 120.51, 110.00, 55.83, 47.06 (2C), 24.18 (2C). UPLC $t_R$ = 2.60 min; HRMS (ESI) $m/z$ calcd for $C_{19}H_{20}N_2O_2F_3$ 365.1477 $[M + H]^+$, found 365.1485.

*4.1.4.3. 1,4-Diazabicyclo[3.2.2]nonan-4-yl(5-(3-fluorophenyl)furan-2-yl)methanone fumarate (**23**).* The title compound was prepared according to the general procedure from **16** (250 mg, 1.26 mmol, 1 equiv), $Cs_2CO_3$ (2.05 g, 6.28 mmol, 5 equiv), and carbonyl chloride **62e** (363 mg, 1.50 mmol, 1.2 equiv). After standard workup and subsequent reaction with fumaric acid (92 mg, 0.79 mmol, 1 equiv), the crude salt was recrystallized from *i*-PrOH to provide the pure fumarate salt **23** × 1.5 $C_4H_4O_4$ as a light brown solid (180 mg, 46% yield); mp = 181−182 °C. $^1$H NMR (300 MHz, $CD_3OD$): $\delta$ 7.63–7.58 (m, 1H), 7.56–7.41 (m, 2H), 7.21 (d, $J$ = 3.6 Hz, 1H), 7.14–7.06 (m, 1H), 7.03 (d, $J$ = 3.6 Hz, 1H), 6.71 (s, 3H), 4.89 (s, br 1H), 4.30 (s, br 2H), 3.57 (dt, $J$ = 15.9, 7.4 Hz, 6H), 2.50–2.17 (m, 4H). $^{13}$C NMR (75 MHz, $CD_3OD$): $\delta$ 170.46 (2C), 164.54 (d, $J$ = 244.9 Hz), 160.68, 156.06, 147.62, 135.89 (2C), 132.98 (d, $J$ = 9.6 Hz), 132.06 (d, $J$ = 8.5 Hz), 121.43 (d, $J$ = 2.9 Hz), 120.69, 116.50 (d, $J$ = 21.5 Hz), 112.16 (d, $J$ = 24.1 Hz), 109.05, 56.08, 46.93, 23.70. UPLC $t_R$ = 2.44 min; HRMS (ESI) $m/z$ calcd for $C_{18}H_{20}N_2O_2F$ 315.1509 $[M + H]^+$, found 315.1511.

*4.1.4.4. 1,4-Diazabicyclo[3.2.2]nonan-4-yl(5-(3-chlorophenyl)furan-2-yl)methanone fumarate (**24**).* The title compound was prepared according to the general procedure from **16** (250 mg, 1.26 mmol, 1 equiv), $Cs_2CO_3$ (2.05 g, 6.28 mmol, 5 equiv), and carbonyl chloride **62f** (338 mg, 1.51

mmol, 1.2 equiv). After standard workup and subsequent reaction with fumaric acid (104 mg, 0.90 mmol, 1 equiv), the crude salt was recrystallized from *i*-PrOH to provide the pure fumarate salt **24** × 0.75 $C_4H_4O_4$ as a light brown solid (320 mg, 80% yield); mp = 186−188 °C. $^1$H NMR (300 MHz, $CD_3OD$): $\delta$ 7.80 (s, 1H), 7.72 (d, *J* = 7.7 Hz, 1H), 7.44 (t, *J* = 7.9 Hz, 1H), 7.40–7.33 (m, 1H), 7.21 (d, *J* = 3.6 Hz, 1H), 7.04 (d, *J* = 3.7 Hz, 1H), 6.70 (s, 1.5H), 4.88 (s, br 1H under water), 4.28 (s, br 2H), 3.54 (dt, *J* = 16.0, 7.4 Hz, 6H), 2.49–2.14 (m, 4H). $^{13}$C NMR (75 MHz, $CD_3OD$): $\delta$ 170.99 (2C), 160.73, 155.80, 147.79, 136.08, 136.04 (2C), 132.71, 131.70, 129.71, 125.31, 123.86, 120.56, 109.11, 55.85, 47.00, 24.13. UPLC $t_R$ = 2.52 min; HRMS (ESI) *m*/*z* calcd for $C_{18}H_{20}N_2O_2Cl$ 331.1213 $[M + H]^+$, found 331.1219.

*4.1.4.5. 1,4-Diazabicyclo[3.2.2]nonan-4-yl(5-(3-bromophenyl)furan-2-yl)methanone fumarate (**25**)*. The title compound was prepared according to the general procedure from **16** (200 mg, 1.0 mmol, 1 equiv), $Cs_2CO_3$ (1.64 g, 5.02 mmol, 5 equiv), and carbonyl chloride **62g** (344 mg, 1.21 mmol, 1.2 equiv). After standard workup and subsequent reaction with fumaric acid (63 mg, 0.54 mmol, 1 equiv), the crude salt was recrystallized from MeOH/$Et_2O$ (4:1) to provide the pure fumarate salt **25** × 1.5 $C_4H_4O_4$ as a light brown solid (161 mg, 43% yield); mp = 204−205 °C. $^1$H NMR (300 MHz, $CD_3OD$): $\delta$ 7.92 (s, 1H), 7.73 (d, *J* = 7.8 Hz, 1H), 7.50 (d, *J* = 8.2 Hz, 1H), 7.35 (t, *J* = 7.9 Hz, 1H), 7.19 (d, *J* = 3.5 Hz, 1H), 7.01 (d, *J* = 3.6 Hz, 1H), 6.71 (s, 3H), 4.88 (s, br 1H), 4.30 (s, br 2H), 3.57 (dt, *J* = 15.1, 6.7 Hz, 6H), 2.49–2.17 (m, 4H). $^{13}$C NMR (75 MHz, $CD_3OD$): $\delta$ 170.48 (2C), 160.74, 155.68, 147.78, 135.91 (2C), 132.93, 132.71, 131.91, 128.25, 124.28, 124.03, 120.60, 109.12, 56.10, 47.05, 24.20. UPLC $t_R$ = 2.54 min; HRMS (ESI) *m*/*z* calcd for $C_{18}H_{20}N_2O_2Br$ 375.0708 $[M + H]^+$, found 375.0705 and 377.0686 (bromine isotope).

*4.1.4.6. 1,4-Diazabicyclo[3.2.2]nonan-4-yl(5-(3-iodophenyl)furan-2-yl)methanone fumarate (**26**)*. The title compound was prepared according to the general procedure from **16** (90 mg, 0.45 mmol, 1 equiv), $Cs_2CO_3$ (736 mg, 2.26 mmol, 5 equiv), carbonyl chloride **62h** (180 mg, 0.54 mmol, 1.2 equiv). After standard workup and subsequent reaction with fumaric acid (92 mg, 0.79 mmol, 1 equiv), the crude salt was recrystallized from MeOH/$Et_2O$ (4:1) to provide the pure fumarate salt **26** × $C_4H_4O_4$ as a light brown solid (150 mg, 53% yield); mp = 184−187 °C. $^1$H NMR (300 MHz, $CD_3OD$): $\delta$ 8.16 (s, 1H), 7.79 (d, *J* = 7.8 Hz, 1H), 7.73 (d, *J* = 7.9 Hz, 1H), 7.28–7.16 (m, 2H), 7.03 (d, *J* = 3.6 Hz, 1H), 6.71 (s, 2H), 4.83 (s, br 1H), 4.28 (s, br 2H), 3.64–3.38 (m, 6H), 2.51–2.11 (m, 4H). $^{13}$C NMR (75 MHz, $CD_3OD$): $\delta$ 170.54 (2C), 160.77, 155.56, 147.77, 138.82, 135.91 (2C), 134.25, 132.86, 131.85, 124.78, 120.57, 108.96, 95.30, 55.96, 47.07, 24.28. UPLC $t_R$ = 2.58 min; HRMS (ESI) *m*/*z* calcd for $C_{18}H_{20}N_2O_2I$ 423.0569 $[M + H]^+$, found 423.0570.

*4.1.4.7. 1,4-Diazabicyclo[3.2.2]nonan-4-yl(5-(3-hydroxyphenyl)furan-2-yl)methanone fumarate (**27**).* The title compound was prepared according to the general procedure from **16** (200 mg, 1.0 mmol, 1 equiv), $Cs_2CO_3$ (1.64 g, 5.02 mmol, 5 equiv), and carbonyl chloride **62i** (268 mg, 1.21 mmol, 1.2 equiv). After standard workup and subsequent reaction with fumaric acid (67 mg, 0.58 mmol, 1 equiv), the crude salt was recrystallized from MeOH/$Et_2O$ (4:1) to provide the pure fumarate salt **27** × 0.5 $C_4H_4O_4$ as a light brown solid (100mg, 40% yield); mp = 231−233 °C. $^1$H NMR (300 MHz, $CD_3OD$): $\delta$ 7.29–7.22 (m, 2H), 7.20–7.14 (m, 2H), 6.88 (d, $J$ = 3.6 Hz, 1H), 6.82–6.76 (m, 1H), 6.69 (s, 1H), 4.84 (s, br 1H under water), 4.22 (s, br 2H), 3.48–3.34 (m, 6H), 2.43–2.07 (m, 4H). $^{13}$C NMR (75 MHz, $CD_3OD$): $\delta$ 171.76 (2C), 160.95, 159.18, 157.66, 147.38, 136.28 (2C), 132.10, 131.18, 120.68 116.98, 116.89, 112.12, 107.80, 56.53, 47.10, 25.33. UPLC $t_R$ = 2.26 min; HRMS (ESI) $m/z$ calcd for $C_{18}H_{21}N_2O_3$ 313.1552 $[M + H]^+$, found 313.1548.

*4.1.4.8. 1,4-Diazabicyclo[3.2.2]nonan-4-yl(5-(3-aminophenyl)furan-2-yl)methanone fumarate (**28**).* The title compound was prepared according to the general procedure from **16** (180 mg, 0.90 mmol, 1 equiv), $Cs_2CO_3$ (1.47 g, 4.52 mmol, 5 equiv), and carbonyl chloride **62l** (240 mg, 1.08 mmol, 1.2 equiv). After standard workup and subsequent reaction with fumaric acid (65 mg, 0.56 mmol, 1 equiv), the crude salt was recrystallized from MeOH/$Et_2O$ (4:1) to provide the pure fumarate salt **28** × 0.75 $C_4H_4O_4$ as a light brown solid (100 mg, 42% yield); mp = 217−219 °C. $^1$H NMR (300 MHz, $CD_3OD$): $\delta$ 7.20–7.05 (m, 4H), 6.84 (d, $J$ = 3.6 Hz, 1H), 6.74–6.70 (m, 1H), 6.69 (s, 1.5H), 4.89 (s, br 1H), 4.24 (s, br 2H), 3.49 (dt, $J$ = 15.7, 6.9 Hz, 6H), 2.46–2.13 (m, 4H). $^{13}$C NMR (75 MHz, $CD_3OD$): $\delta$ 171.43 (2C), 160.94, 158.21, 149.95, 147.03, 136.18 (2C), 131.52, 130.74, 120.94, 117.00, 115.23, 111.89, 107.48, 56.50, 47.09, 25.00. UPLC $t_R$ = 2.45 min; HRMS (ESI) $m/z$ calcd for $C_{18}H_{22}N_3O_2$ 312.1712 $[M + H]^+$, found 312.1705.

*4.1.4.9. 1,4-Diazabicyclo[3.2.2]nonan-4-yl(5-(3-nitrophenyl)furan-2-yl)methanone fumarate (**29**).* The title compound was prepared according to the general procedure from **16** (120 mg, 0.6 mmol, 1 equiv), $Cs_2CO_3$ (970 mg, 3 mmol, 5 equiv), and carbonyl chloride **62m** (180 mg, 0.75 mmol, 1.2 equiv). After standard workup and subsequent reaction with fumaric acid (50 mg, 0.40 mmol, 1 equiv), the crude salt was recrystallized from MeOH to provide the pure fumarate salt **29** × $C_4H_4O_4$ as a yellow solid (100 mg, 50% yield); mp = 202−205 °C. $^1$H NMR (300 MHz, $CD_3OD$): $\delta$ 8.60 (t, $J$ = 1.8 Hz, 1H), 8.28–8.11 (m, 2H), 7.71 (t, $J$ = 8.0 Hz, 1H), 7.24 (d, $J$ = 3.4 Hz, 1H), 7.19 (d, $J$ = 3.7 Hz, 1H), 6.69 (s, 2H), 4.89 (s, br 1H), 4.28 (s, br 2H), 3.52 (dt, $J$ = 14.4, 6.5 Hz, 6H), 2.49–2.12 (m, 4H). $^{13}$C NMR (75 MHz, DMSO-$d_6$): $\delta$ 167.08 (2C), 158.01, 148.45 (2C), 147.76, 134.54 (2C), 130.86, 130.79, 130.11, 122.79, 118.32, 117.35, 109.51, 55.84, 48.59, 45.23 (2C), 26.09, 24.74 (2C). UPLC $t_R$ = 2.41 min; HRMS (ESI) $m/z$ calcd for $C_{18}H_{20}N_3O_4$ 342.1454 $[M + H]^+$, found 342.1460.

*4.1.4.10. [2,3'-Bifuran]-5-yl(1,4-diazabicyclo[3.2.2]nonan-4-yl)methanone fumarate* (**30**). The title compound was prepared according to the general procedure from **16** (150 mg, 0.75 mmol, 1 equiv), $Cs_2CO_3$ (1.20 g, 3.7 mmol, 5 equiv), and carbonyl chloride **63** (175 mg, 0.89 mmol, 1.2 equiv). After standard workup and subsequent reaction with fumaric acid (40 mg, 0.35 mmol, 1 equiv), the crude salt was recrystallized from MeOH/EtOH/$Et_2O$ (4:2:1) to provide the pure fumarate salt **30** × 0.5 $C_4H_4O_4$ as a white solid (80 mg, 57% yield); mp = 176−178 °C. $^1$H NMR (300 MHz, $CD_3OD$): $\delta$ 7.99 (s, 1H), 7.62–7.57 (m, 1H), 7.16 (d, $J$ = 3.5 Hz, 1H), 6.80–6.77 (m, 1H), 6.70 (s, 1H), 6.67 (d, $J$ = 3.6 Hz, 1H), 4.86 (s, br 1H), 4.25 (s, br 2H), 3.55 (dt, $J$ = 15.7, 6.8 Hz, 6H), 2.47–2.15 (m, 4H). $^{13}$C NMR (75 MHz, $CD_3OD$): $\delta$ 171.34 (2C), 160.75, 151.78, 146.49, 145.53, 141.15, 136.12 (2C), 120.50, 118.30, 108.73, 107.87, 55.66, 46.92, 24.39. UPLC $t_R$ = 2.26 min; HRMS (ESI) $m/z$ calcd for $C_{16}H_{19}N_2O_3$ 287.1396 $[M + H]^+$, found 287.1393.

*4.1.4.11. 1,4-Diazabicyclo[3.2.2]nonan-4-yl(5-(naphthalen-2-yl)furan-2-yl)methanone fumarate (**31**)*. The title compound was prepared according to the general procedure from **16** (160 mg, 0.80 mmol, 1 equiv), $Cs_2CO_3$ (1.30 g, 4 mmol, 5 equiv), and carbonyl chloride **64** (250 mg, 0.97 mmol, 1.2 equiv). After standard workup and subsequent reaction with fumaric acid (54 mg, 0.46 mmol, 1 equiv), the crude salt was recrystallized from MeOH to provide the pure fumarate salt **31** × $C_4H_4O_4$ as a white solid (95 mg, 45% yield); mp = 179−181 °C. $^1$H NMR (300 MHz, $CD_3OD$): $\delta$ 8.38–8.29 (m, 1H), 8.00–7.93 (m, 2H), 7.82 (dd, $J$ = 7.2, 0.9 Hz, 1H), 7.64–7.52 (m, 3H), 7.34 (d, $J$ = 3.4 Hz, 1H), 6.99 (d, $J$ = 3.6 Hz, 1H), 6.70 (s, 2H), 4.93 (s, br 1H), 4.29 (s, br 2H), 3.56–3.40 (m, 6H), 2.45–2.11 (m, 4H). $^{13}$C NMR (75 MHz, $CD_3OD$): $\delta$ 170.77 (2C), 160.96, 157.06, 148.00, 136.00 (2C), 135.49, 131.56, 130.96, 129.86, 128.46, 128.22, 128.17, 127.39, 126.39 (2C), 125.92, 112.11, 56.57, 47.17, 24.86. UPLC $t_R$ = 2.58 min; HRMS (ESI) $m/z$ calcd for $C_{22}H_{23}N_2O_2$ 347.1760 $[M + H]^+$, found 347.1761.

*4.1.4.12. 1,4-Diazabicyclo[3.2.2]nonan-4-yl(5-(isoquinolin-4-yl)furan-2-yl)methanone fumarate (**32**)*. The title compound was prepared according to the general procedure from **16** (84 mg, 0.42 mmol, 1 equiv), $Cs_2CO_3$ (700 mg, 2 mmol, 5 equiv), and carbonyl chloride **65** (130 mg, 0.50 mmol, 1.2 equiv). After standard workup, the residue was diluted with *n*-hexane to obtain a suspension, from which the solvent was removed to afford the free base **32** as light brown semi-solid (20 mg, 30% yield). $^1$H NMR (300 MHz, $CD_3OD$): $\delta$ 8.91 (s, 1H), 8.45 (s, 1H), 8.04 (d, $J$ = 8.4 Hz, 1H), 7.72 (d, $J$ = 7.7 Hz, 1H), 7.52–7.42 (m, 1H), 7.40–7.30 (m, 1H), 6.86 (s, br 1H), 6.57 (d, $J$ = 3.5 Hz, 1H), 4.43 (s, br 1H), 3.69 (s, br 2H), 2.90–2.45 (m, 6H), 1.91–1.70 (m, 2H), 1.59–1.37 (m, 2H). $^{13}$C NMR (75 MHz, $CD_3OD$): $\delta$ 160.94, 154.08, 153.36, 149.38, 142.60, 133.66, 133.41, 129.96, 129.83, 129.36, 125.22, 123.13, 118.69, 112.84, 60.13, 57.89, 46.87 (2C), 33.07, 26.95

(2C). UPLC $t_R$ = 2.20 min; HRMS (ESI) *m/z* calcd for $C_{21}H_{22}N_3O_2$ 348.1712 $[M + H]^+$, found 348.1713.

*4.2. Electrophysiology*

Human nAChR clones obtained from Dr. Jon Lindstrom (University of Pennsylvania, Philadelphia PA) were used to heterologously express human AChRs in *Xenopus laevis* oocytes. The RIC-3 clone (human resistance-to-cholinesterase 3) was obtained from Dr. Millet Treinin (Hebrew University, Israel) and was co-injected with α7 to improve the level and speed of α7 receptor expression without affecting the pharmacological properties of the receptors [53]. Upon linearization and purification of the plasmid cDNAs, cRNAs were prepared using the mMessage mMachine in vitro RNA transcription kit (Ambion, Austin, TX). Oocytes were surgically removed from mature *Xenopus laevis* frogs (Nasco, Ft. Atkinson WI) and injected with appropriate nAChR subunit cRNAs as described previously [51]. Frogs were maintained in the Animal Care Service facility of the University of Florida, and all procedures were approved by the University of Florida Institutional Animal Care and Use Committee and have been previously described [31]. Two-electrode voltage-clamp electrophysiology experiments were conducted using OpusXpress 6000A (Molecular Devices, Union City, CA) [51]. Both the voltage and current electrodes were filled with 3 M KCl. Oocytes were voltage-clamped at -60 mV. The oocytes were bath-perfused with Ringer's solution (115 mM NaCl, 2.5 mM KCl, 1.8 mM $CaCl_2$, 10 mM HEPES, and 1 μM atropine, pH 7.2) at 2 mL/min for α7 nAChR. The test solutions were applied from 96-well plates via disposable tips. Drug applications were 12 s in duration followed by a 181 s washout period for α7 nAChR. Acetylcholine chloride (ACh), used as control at 60 μM prepared freshly in Ringer's solution each day, was purchased from Sigma-Aldrich Chemical Company (St. Louis, MO). To evaluate the effects of experimental compounds compared to ACh-evoked responses of α7 nAChR subtype expressed in oocytes, control responses were defined as the average of two initial applications of ACh made before test applications, which were then normalized to the control responses of each oocyte. The responses were collected as both peak current amplitudes and net charge as previously described [51]. Data were collected at 50 Hz, filtered at 20 Hz for α7, and analyzed by Clampfit 10.3 (Molecular Devices) and Excel (Microsoft, Redmond WA). Data are expressed as means ± SEM (standard errors of the mean) from at least four oocytes for each experiment and plotted by Kaleidagraph 4.1 (Abelbeck Software, Reading, PA). For Fig. 3, following subtraction of the basal holding current, data from each cell, including the ACh controls, were normalized by dividing each of the 10,322 points in each of the 206.44 s traces (acquired at 50 Hz) by the peak of the ACh control from the same cell. The normalized data were then averaged and standard errors of the

mean (SEM) for the multi-cell averages calculated on a point-by-point basis. Comparisons of results were made using *t*-tests between the groups of experimental values. The value of $P < 0.05$ was used to constitute the level of significance. The statistics were calculated using an Excel template provided in Microsoft Office.

All the compounds were assayed for activity with the human α7 nAChR expressed in *Xenopus* oocytes using two-electrode voltage clamping and applying two protocols. The protocol I employed two initial 60 μM ACh pre-control applications to normalize the subsequent responses for each oocyte. Then the lead compound **1** was tested at 1, 3, 10, 30 μM, whereas derivatives **11-32** were tested at 10 μM. This concentration provided a standard comparison benchmark, giving an observable response while avoiding possible complications such as channel block. A 60 μM ACh post-control was delivered to determine the receptor desensitization and followed by 10 μM of the type II PAM PNU-120596 to detect residual receptor response potentiation. Last, a 60 μM ACh post-control was applied to further evaluate residual inhibition or potentiation. The protocol II employed application of two initial 60 μM ACh pre-controls to normalize the subsequent responses, followed by compounds applied at 1, 3, 10, and 30 μM for **1** and 10 μM for **11-32** co-applied with 10 μM of PNU-120596, to determine the direct potentiation of the response to the test compound. Last, a 60 μM ACh post-control application indicated residual inhibition or potentiation of the receptor. The concentration–response curves of compounds **13** and **17** were obtained by applying two initial 60 μM ACh pre-controls followed by drug applications that alternated between experimental compound at 0.1, 0.3, 1, 3, 10, and 30 μM and 60 μM ACh controls.

## Declaration of competing interest

The authors declare that they have no known competing financial interests or personal relationships that could have appeared to influence the work reported in this paper.

## Acknowledgments

This research was financially supported by National Institute of Health grant GM57481. The University of Milan financed the doctoral position of M.C.P.

## Appendix A. Supplementary data

Supplementary data to this article can be found online.

## References


[1] S. Couturier, D. Bertrand, J.M. Matter, M.C. Hernandez, S. Bertrand, N. Millar, S. Valera, T. Barkas, M. Ballivet, A neuronal nicotinic acetylcholine-receptor subunit (Alpha-7) is developmentally regulated and forms a homooligomeric channel blocked by alpha-btx, Neuron. 5 (1990) 847−856. https://doi.org/10.1016/0896-6273(90)90344-F.

[2] P. Seguela, J. Wadiche, K. Dineley-Miller, J.A. Dani, J.W. Patrick, Molecular cloning, functional properties, and distribution of rat brain alpha7: a nicotinic cation channel highly permeable to calcium, J. Neurosci. 13 (1993) 596−604. https://doi.org/10.1523/JNEUROSCI.13-02-00596.1993.

[3] B. Lendvai, F. Kassai, A. Szájli, Z. Némethy, α7 Nicotinic acetylcholine receptors and their role in cognition, Brain Res. Bull. 93 (2013) 86−96. https://doi.org/10.1016/j.brainresbull.2012.11.003.

[4] C. Gotti, F. Clementi, Neuronal nicotinic receptors: from structure to pathology, Prog. Neurobiol. 74 (2004) 363−396. https://doi.org/10.1016/j.pneurobio.2004.09.006.

[5] T. Fujii, M. Mashimo, Y. Moriwaki, H. Misawa, S. Ono, K. Horiguchi, K. Kawashima, Expression and function of the cholinergic system in immune cells, Front. Immunol. 8 (2017) 1085. https://doi.org/10.3389/fimmu.2017.01085.

[6] C.A. Báez-Pagán, M. Delgado-Vélez, J.A. Lasalde-Dominicci, Activation of the macrophage α7 nicotinic acetylcholine receptor and control of inflammation, J. Neuroimmune Pharmacol. 10 (2015) 468−476. https://doi.org/10.1007/s11481-015-9601-5.

[7] D.K, Williams, C. Peng, M.R. Kimbrell, R.L. Papke, Intrinsically low open probability of α7 nicotinic acetylcholine receptors can be overcome by positive allosteric modulation and serum factors leading to the generation of excitotoxic currents at physiological temperatures, Mol. Pharmacol. 82 (2012) 746−759. https://doi.org/10.1124/mol.112.080317.

[8] K. Pesti, A.K. Szabo, A. Mike, E.S. Vizi, Kinetic properties and open probability of α7 nicotinic acetylcholine receptors, Neuropharmacology 81 (2014) 101−115. https://doi.org/10.1016/j.neuropharm.2014.01.034.

[9] D.K. Williams, J. Wang, R.L. Papke, Investigation of the molecular mechanism of the α7 nicotinic acetylcholine receptor positive allosteric modulator PNU-120596 provides evidence for two distinct desensitized states, Mol. Pharmacol. 80 (2011) 1013−1032. https://doi.org/10.1124/mol.111.074302.

[10] C. Zhong, D.A. Talmage, L.W. Role, Nicotine elicits prolonged calcium signaling along ventral hippocampal axons, PLoS One 8 (2013) e82719. https://doi.org/10.1371/journal.pone.0082719.

[11] J.C. Nordman, N. Kabbani, Microtubule dynamics at the growth cone are mediated by α7

nicotinic receptor activation of a Gαq and $IP_3$ receptor pathway, FASEB J. 28 (2014) 2995−3006. https://doi.org/10.1096/fj.14-251439.

[12] J.O. Colón-Sáez, J.L. Yakel, A mutation in the extracellular domain of the α7 nAChR reduces calcium permeability, Pflugers Arch. 466 (2014) 1571−1579. https://doi.org/10.1007/s00424-013-1385-y.

[13] C. Stokes, M. Treinin, R.L. Papke, Looking below the surface of nicotinic acetylcholine receptors, Trends Pharmacol. Sci. 36 (2015) 514−523. https://doi.org/10.1016/j.tips.2015.05.002.

[14] R.L. Papke, Merging old and new perspectives on nicotinic acetylcholine receptors, Biochem. Pharmacol. 89 (2014) 1−11. https://doi.org/10.1016/j.bcp.2014.01.029.

[15] N. Kabbani, R.A. Nichols, Beyond the channel: metabotropic signaling by nicotinic receptors, Trends Pharmacol. Sci. 39 (2018) 354−366. https://doi.org/10.1016/j.tips.2018.01.002.

[16] W.T. de Jonge, L. Ulloa, The alpha7 nicotinic acetylcholine receptor as a pharmacological target for inflammation, Br. J. Pharmacol. 151 (2007) 915−929. https://doi.org/10.1038/sj.bjp.0707264.

[17] M. Treinin, R.L. Papke, E. Nizri, Y. Ben-David, T. Mizrachi, T. Brenner, Role of the α7 nicotinic acetylcholine receptor and RIC-3 in the cholinergic anti-inflammatory pathway, Cent. Nerv. Syst. Agents Med. Chem. 17 (2017) 90−99. https://doi.org/10.2174/1871524916666160829114533.

[18] M. Rosas-Ballina, R.S. Goldstein, M. Gallowitsch-Puerta, L. Yang, S.I. Valdés-Ferrer, N.B. Patel, S. Chavan, Y. Al-Abed, H. Yang, K.J. Tracey, The selective α7 agonist GTS-21 attenuates cytokine production in human whole blood and human monocytes activated by ligands for TLR2, TLR3, TLR4, TLR9, and RAGE, Mol. Med. 15 (2009) 195−202. https://doi.org/10.2119/molmed.2009.00039.

[19] M.S. Thomsen, J.D. Mikkelsen, The α7 nicotinic acetylcholine receptor ligands methyllycaconitine, NS6740 and GTS-21 reduce lipopolysaccharide-induced TNF-α release from microglia, J. Neuroimmunol. 251 (2012) 65−72. https://doi.org/10.1016/j.jneuroim.2012.07.006.

[20] J.A. Paulo, W.J. Brucker, E. Hawrot, Proteomic analysis of an α7 nicotinic acetylcholine receptor interactome, J. Proteome Res. 8 (2009) 1849−1858. https://doi.org/10.1021/pr800731z.

[21] J.R. King, J.C. Nordman, S.P. Bridges, M.K. Lin, N. Kabbani, Identification and characterization of a G protein-binding cluster in α7 nicotinic acetylcholine receptors, J. Biol. Chem. 290 (2015) 20060−20070. https://doi.org/10.1074/jbc.M115.647040.

[22] J.R. King, T.C. Gillevet, N.A. Kabbani, G protein-coupled α7 nicotinic receptor regulates

signaling and TNF-α release in microglia, FEBS Open Bio 7 (2017) 1350−1361. https://doi.org/10.1002/2211-5463.12270.

[23] K.J. Tracey, Physiology and immunology of the cholinergic antiinflammatory pathway, J. Clin. Invest. 117 (2007) 289−296. https://doi.org/10.1172/JCI30555.

[24] J. Corradi, C. Bouzat, Understanding the bases of function and modulation of α7 nicotinic receptors: implications for drug discovery, Mol. Pharmacol. 90 (2016) 288−299. https://doi.org/10.1124/mol.116.104240.

[25] N.A. Horenstein, R.L. Papke, Anti-inflammatory silent agonists, ACS Med. Chem. Lett. 8 (2017) 989−991. https://doi.org/10.1021/acsmedchemlett.7b00368.

[26] R.L. Papke, D. Bagdas, A.R. Kulkarni, T. Gould, S.D. AlSharari, G.A. Thakur, M.I. Damaj, The analgesic-like properties of the alpha7 nAChR silent agonist NS6740 is associated with non-conducting conformations of the receptor, Neuropharmacology 91 (2015) 34−42. https://doi.org/10.1016/j.neuropharm.2014.12.002.

[27] M. Quadri, D. Bagdas, W. Toma, C. Stokes, N.A. Horenstein, M.I. Damaj, R.L. Papke, The antinociceptive and anti-inflammatory properties of the α7 nAChR weak partial agonist p-$CF_3$ N,N-diethyl-N'-phenylpiperazine, J. Pharmacol. Exp. Ther. 367 (2018) 203−214. https://doi.org/10.1124/jpet.118.249904.

[28] C.A. Briggs, J.H. Grønlien, P.Curzon, D.B. Timmermann, H. Ween, K. Thorin-Hagene, P. Kerr, D.J. Anderson, J. Malysz, T. Dyhring, G.M. Olsen, D. Peters, W.H. Bunnelle, M. Gopalakrishnan, Role of channel activation in cognitive enhancement mediated by α7 nicotinic acetylcholine receptors, Br. J. Pharmacol. 158 (2009) 1486−1494. https://doi.org/10.1111/j.1476-5381.2009.00426.x.

[29] K. Chojnacka, R.L. Papke, N.A. Horenstein, Synthesis and evaluation of a conditionally-silent agonist for the α7 nicotinic acetylcholine receptor, Bioorg. Med. Chem. Lett. 23 (2013) 4145−4149. https://doi.org/10.1016/j.bmcl.2013.05.039.

[30] R.B. Clark, D. Lamppu, L. Libertine, A. McDonough, A. Kumar, G. LaRosa, R. Rush, D. Elbaum, Discovery of novel 2-((pyridin-3-yloxy)methyl)piperazines as α7 nicotinic acetylcholine receptor modulators for the treatment of inflammatory disorders, J. Med. Chem. 57 (2014) 3966−3983. https://doi.org/10.1021/jm5004599.

[31] R.L. Papke, K. Chojnacka, N.A. Horenstein, The minimal pharmacophore for silent agonism of the α7 nicotinic acetylcholine receptor, J. Pharmacol. Exp. Ther. 650 (2014) 665−680. https://doi.org/10.1124/jpet.114.215236.

[32] M. Quadri, R.L. Papke, N.A. Horenstein, Dissection of N,N-diethyl-N'-phenylpiperazines as α7 nicotinic receptor silent agonists, Bioorg. Med. Chem. 24 (2016) 286−293. https://doi.org/10.1016/j.bmc.2015.12.017.

[33] M. Quadri, C. Stokes, A. Gulsevin, A.C.J. Felts, K.A. Abboud, R.L. Papke, N.A. Horenstein,

A. Sulfonium as a surrogate for ammonium: a new α7 nicotinic acetylcholine receptor partial agonist with desensitizing activity, J. Med. Chem. 60 (2017) 7928−7934. https://doi.org/10.1021/acs.jmedchem.7b00875.

[34] M. Quadri, C. Matera, A. Silnović, M.C. Pismataro, N.A. Horenstein, C. Stokes, R.L. Papke, C. Dallanoce, Identification of α7 nicotinic acetylcholine receptor silent agonists based on the spirocyclic quinuclidine-$\Delta^2$-isoxazoline scaffold: synthesis and electrophysiological evaluation, ChemMedChem 12 (2017) 1335−1348. https://doi.org/10.1002/cmdc.201700162.

[35] M. Quadri, A. Silnović, C. Matera, N.A. Horenstein, C. Stokes, M. De Amici, R.L. Papke, C. Dallanoce, Novel 5-(quinuclidin-3-ylmethyl)-1,2,4-oxadiazoles to investigate the activation of the α7 nicotinic acetylcholine receptor subtype: synthesis and electrophysiological evaluation, Eur. J. Med. Chem. 160 (2018) 207−228. https://doi.org/10.1016/j.ejmech.2018.10.015.

[36] R.L. Papke, C. Stokes, M.I. Damaj, G.A. Thakur, K. Manther, M. Treinin, D. Bagdas, A.R. Kulkarni, N.A. Horenstein, Persistent activation of α7 nicotinic ACh receptors associated with stable induction of different desensitized states, Br. J. Pharmacol. 175 (2018) 1838−1854. https://doi.org/10.1111/bph.13851.

[37] A. Gulsevin, R.L. Papke, C. Stokes, S. Garai, G.A. Thakur, M. Quadri, N.A. Horenstein, Allosteric Agonism of α7 Nicotinic Acetylcholine Receptors: Receptor Modulation Outside the Orthosteric Site, Mol. Pharmacol. 95 (2019) 606−614. https://doi.org/10.1124/mol.119.115758.

[38] C. Dallanoce, P. Magrone, C. Matera, F. Frigerio, G. Grazioso, M. De Amici, S. Fucile, V. Piccari, K. Frydenvang, L. Pucci, C. Gotti, F. Clementi, C. De Micheli, Design, synthesis and pharmacological characterization of novel spirocyclic quinuclidinyl-$\Delta^2$-isoxazoline derivatives as potent and selective agonists of α7 nicotinic acetylcholine receptors, ChemMedChem 6 (2011) 889−903. https://doi.org/10.1002/cmdc.201000514.

[39] C. Dallanoce, F. Frigerio, G. Grazioso, C. Matera, G.L. Visconti, M. De Amici, L. Pucci, F. Pistillo, S. Fucile, C. Gotti, F. Clementi, C. De Micheli, New spirocyclic $\Delta^2$-isoxazoline derivatives related to selective agonists of α7 neuronal nicotinic acetylcholine receptors, Eur. J. Med. Chem. 46 (2011) 5790−5799. https://doi.org/10.1016/j.ejmech.2011.09.028.

[40] L. Di Cesare Mannelli, A. Pacini, C. Matera, M. Zanardelli, T. Mello, M. De Amici, C. Dallanoce, C. Ghelardini, Involvement of α7 nAChR subtype in rat oxaliplatin-induced neuropathy: effects of selective activation, Neuropharmacology 79 (2014) 37−48. https://doi.org/10.1016/j. neuropharm.2013.10.034.

[41] C. Matera, G. Dondio, D. Braida, L. Ponzoni, M. De Amici, M. Sala, C. Dallanoce, In vivo and in vitro ADMET profiling and in vivo pharmacodynamic investigations of a selective

α7 nicotinic acetylcholine receptor agonist with a spirocyclic $\Delta^2$-isoxazoline molecular skeleton, Eur. J. Pharmacol. 820 (2018) 265−273. https://doi.org/10.1016/j.ejphar.2017.12.047.

[42] G. Scabia, R. Cancello, C. Dallanoce, S. Berger, C. Matera, A. Dattilo, A. Zulian, I. Barone, G. Ceccarini, F. Santini, M. De Amici, A.M. Di Blasio, M. Maffei, ICH3, a selective alpha7 nicotinic acetylcholine receptor agonist, modulates adipocyte inflammation associated with obesity, J. Endocrinol. Invest. Published Online: January 21, 2020. https://doi.org/10.1007/s40618-020-01182-z.

[43] G. Grazioso, D.Y. Pomè, C. Matera, F. Frigerio, L. Pucci, C. Gotti, C. Dallanoce, M. De Amici, Design of novel α7-subtype-preferring nicotinic acetylcholine receptor agonists: application of docking and MM-PBSA computational approaches, synthetic and pharmacological studies, Bioorg. Med. Chem. Lett. 19 (2009) 6353−6357. https://doi.org/10.1016/j.bmcl.2009.09.073.

[44] C. Dallanoce, C. Matera, L. Pucci, C. Gotti, F. Clementi, M. De Amici, C. De Micheli, Synthesis and binding affinity at α4β2 and α7 nicotinic acetylcholine receptors of new analogues of epibatidine and epiboxidine containing the 7-azabicyclo[2.2.1]hept-2-ene ring system, Bioorg. Med. Chem. Lett. 22 (2012) 829−832. https://doi.org/10.1016/j.bmcl.2011.12.052.

[45] C. Dallanoce, G. Grazioso, D.Y. Pomè, M. Sciaccaluga, C. Matera, C. Gotti, S. Fucile, M. De Amici, Investigating the hydrogen-bond acceptor site of the nicotinic pharmacophore model: a computational and experimental study using epibatidine-related molecular probes, J. Comput. Aided Mol. Des. 27 (2013) 975−987. https://doi.org/10.1007/s10822-013-9694-y.

[46] C. Matera, M. Quadri, M. Sciaccaluga, D.Y. Pomè, F. Fasoli, M. De Amici, S. Fucile, C. Gotti, C. Dallanoce, G. Grazioso, Modification of the anabaseine pyridine nucleus allows achieving binding and functional selectivity for the α3β4 nicotinic acetylcholine receptor subtype, Eur. J. Med. Chem. 108 (2016) 392−405. https://doi.org/10.1016/j.ejmech.2015.11.045.

[47] D. Peters, G.M. Olsen, E.Ø. Nielsen, T.D. Jørgensen, P.K. Ahring, Novel Diazabicyclic Aryl Derivatives, WO 2004/076453 A1, September 10, 2004.

[48] T.F. Braish, D.E. Fox, Synthesis of (S,S)- and (R,R)-2-Alkyl-2,5-diazabicyclo[2.2.1]heptanes, J. Org. Chem. 55 (1990) 1684−1687. https://doi.org/10.1021/jo00292a054.

[49] S. Lee, K.Y. Yi, S.K. Hwang, B.H. Lee, S. Yoo, K. Lee, (5-Arylfuran-2-ylcarbonyl)guanidines as cardioprotectives through the inhibition of $Na^+/H^+$ exchanger isoform-1, J. Med. Chem. 48 (2005) 2882−2891. https://doi.org/10.1021/jm0492305.

[50] C. Bressy, D. Alberico, M.A. Lautens, A route to annulated indoles via a palladium-catalyzed tandem alkylation/direct arylation reaction, J. Am. Chem. Soc. 127 (2005) 13148−13149. https://doi.org/10.1021/ja054472v.

[51] R.L. Papke, C. Stokes, Working with OpusXpress: methods for high volume oocyte experiments, Methods 51 (2010) 121−133. https://doi.org/10.1016/j.ymeth.2010.01.012.

[52] R.L. Papke, J.K.P. Papke, Comparative pharmacology of rat and human α7 nAChR conducted with net charge analysis, Br. J. Pharmacol. 137 (2002) 49−61. https://doi.org/10.1038/sj.bjp.0704833.

[53] S. Halevi, L. Yassin, M. Eshel, F. Sala, S. Sala, M. Criado, M. Treinin, Conservation within the RIC-3 gene family. Effectors of mammalian nicotinic acetylcholine receptor expression, J. Biol. Chem. 278 (2003) 34411−34417. https://doi.org/10.1074/jbc.M300170200.